Genetic and environmental conditions influencing cellular aggregates formation in *Burkholderia multivorans*

Sara Caracol Gomes

Thesis to obtain the Master of Science Degree in

Microbiology

Supervisor: Doctor Leonilde de Fátima Morais Moreira

Examination Committee:

Chairperson: Doctor Jorge Humberto Gomes Leitão

Supervisor: Doctor Leonilde de Fátima Morais Moreira

Members of the committee: Doctor Arsénio do Carmo Sales Mendes Fialho

November 2018

ACKNOWLEDGMENTS

First of all, I would like to thank to my supervisor Prof. Leonilde Moreira, for all the guidance, help, advices and support during the development of this work. I would also like to thank to every member of the Biological Sciences Research Group (BSRG) who helped me throughout my experimental work. I would like to thank to all my colleagues and friends, that have been with me this entire year, for always making our work days much easier and, for always making the hardest work day more fun. Obviously, I want to thank to my friend Mirela Ferreira for always being there for me, for always laughing and crying with me, for helping raise my head up when giving up looked much easier. Basically, thank you for being the other coccus in our team. Additionally, I want to thank Ana Rita Basílio for always making every day a much funnier day, and always being there with a strength word.

This work was financed by Programa Operacional Regional de Lisboa 2020 (Lisboa-01-0145-FEDER-007317) which is also thankfully acknowledged.

A special thank you to my dearest friend Ana Rita Nogueira, for being with me the past six years. For always being there when a nice word was needed, for always believing and supporting me when I could not do it for myself.

Finally, I would like to thank my family, specially to my parents, for giving me the opportunity to fulfil my dreams, for always supporting and believing in me and, for the endless motivation.

RESUMO

As infeções respiratórias crónicas de origem bacteriana têm um impacto económico muito elevado sobre os sistemas de saúde. Um exemplo destas infecções são as que afectam doentes com fibrose quística, muitas vezes causadas por agentes patogénicos oportunistas como os pertencentes ao complexo *Burkholderia cepacia,* muitas vezes associados a um aumento da morbilidade e da mortalidade. Sabe-se que a transição bacteriana para um estado de infecção crónica é caracterizada por mudanças fenotípicas que se pensa reflectirem a adaptação aos stresses presentes no pulmão destes doentes. Contudo, desconhece-se a forma como estes stresses actuam nas bactérias impulsionando a transição para a infeção crónica. Uma hipótese é que os factores de stresse actuem nas células promovendo a formação de agregados celulares. Para testar esta hipótese, analisaram-se isolados de *Burkholderia multivorans* recolhidos de 9 doentes com fibrose quística, tendo-se confirmado que a maioria produz agregados celulares e a sua quantidade aumenta quando sujeitos a um meio que simula o ambiente pulmonar. A condição que melhor estimula de agregação celular é o crescimento na presença de ciprofloxacina. Relativamente aos mecanismos moleculares envolvidos na agregação celular, confirmou-se que a enzima lactato desidrogenase desempenha um papel importante neste fenómeno. Na tentativa de encontrar outros genes que afectem a agregação celular, realizou-se uma experiência de evolução onde foi possível desenvolver este fenótipo sob condições laboratoriais. A sequenciação do genoma duma dessas colónias levou à identificação de mutações em genes envolvidos na síntese de pili e na degradação de peptidoglicano, podendo estes estar envolvidos na formação destas estruturas multicelulares.

Palavras-chave: Fibrose quística; *Burkholderia multivorans*; agregados celulares; condições de stresse; lactato desidrogenase; evolução experimental

ABSTRACT

Chronic respiratory bacterial infections are a significant healthcare cost. One such case is the respiratory infections of cystic fibrosis patients, often caused by opportunistic pathogens of the *Burkholderia cepacia* complex, which are associated with increasing morbidity and mortality. Bacterial transitions to chronicity are characterized by phenotypic changes, thought to reflect adaptation to stresses of the cystic fibrosis lung. Yet, how these stressors act on bacteria to drive the transition to chronic infection is unknown. We hypothesize that stressors act on cells and trigger the formation of cellular aggregates. To test this hypothesis, we analysed and confirmed that the majority of the *Burkholderia multivorans* isolates recovered from 9 patients do form cell aggregates and this number increases in a medium mimicking the cystic fibrosis lung. Sub-inhibitory concentration of ciprofloxacin was the best trigger of aggregates formation. Regarding putative molecular players in aggregates formation, it was confirmed the role of lactate dehydrogenase enzyme in this process. With the aim of finding additional genes involved in cellular aggregation, an evolution experiment was performed. Not only it was possible to evolve this phenotype under laboratory settings, but by sequencing the whole genome of an evolved colony, we identified genes required for pili synthesis and peptidoglycan degradation as possibly involved in the formation of this multicellular structures.

Keywords: Cystic Fibrosis; *Burkholderia multivorans*; cellular aggregates; stress conditions; lactate dehydrogenase; experimental evolution

LIST OF ABREVIATIONS

ABC	ATP-biding cassette
ASM	Artificial Sputum Medium
ATP	Adenosine Triphosphate
Bcc	*Burkholderia cepacia* complex
CF	Cystic Fibrosis
CFTR	Cystic Fibrosis Transmembrane Conductance Regulator
CoA	Acetyl Coenzyme A
DNA	Deoxyribonucleic Acid
EPS	Extracellular Polymeric Substance (exopolysaccharide)
LB	Luria-Bertani medium
LdhA	Lactate Dehydrogenase
LPS	Lipopolysaccharide
MH	Mueller-Hinton medium
MIC	Minimal Inhibitory Concentration
NAD	Nicotinamide Adenine Dinucleotide
OD	Optical Density
PCR	Polymerase Chain Reaction
PHB	Poly-β-hydroxybutyrate
PQS	*Pseudomonas* Quinolone Signal
RPM	Rotations Per Minute
SCFM	Synthetic Cystic Fibrosis medium
TLR-2	Toll Like Receptor-2
tRNA	Transfer RNA
YEM	Yeast Extract Mannitol medium

LIST OF CONTENTS

LIST OF TABLES

LIST OF FIGURES

1. Introduction

Cystic Fibrosis (CF) patients suffer from permanent polymicrobial lung infections caused by several types of bacteria, including *Pseudomonas aeruginosa*, *Burkholderia cepacia* complex (Bcc) bacteria and bacteria from genera like *Streptococcus, Prevotella, Veillonella, Neisseria, Porphorymonas* and *Catonella* (Filkins and O'Toole 2015). *Pseudomonas* and *Burkholderia*, represent a main problem when colonizing these patients as their strains are highly resistant to antibiotics and other bactericidal agents commonly used as lung infection treatment in CF patients. The synthesis of multidrug efflux pumps, beta-lactamases and exopolysaccharides (EPS) (not only its amount, but also its composition) can explain the antimicrobial resistance observed (Aaron et al. 2000; Ferreira et al. 2011). Due to that, species are able to maintain competitiveness in the environments where colonization is occurring (Bible et al. 2015). It is thought that resistance presented by these species is due to conventional biofilms (a surface attached microbial community embedded in an extracellular matrix composed by EPS and DNA) and cellular aggregates formation, a form of non-attached biofilm (Sriramulu et al. 2005). Some authors divided cellular aggregates in two different types according with its morphology and physiology. These two types are clumps and flocculation. Bible et al., defines clumps as a set of motile bacteria that transiently adhere at their nonflagellated pole by cell-to-cell interaction; and flocculation as a transition of motile to nonmotile cells encased in an exopolysaccharides (EPS) matrix (Bible et al. 2015, 2008; Sadasivan and Neyra 1985). Yet, clumping is a prerequisite to flocculation. This separation inside cellular aggregates concept is not considered by all authors studying this matter. Some research groups do not distinguish cellular aggregates from cell clumps and flocculation. In these cases, cellular aggregates, cell clumps, and flocculation are different possible designations for the same cell aggregation phenomenon.

Due to this, several studies have been developed to understand in which conditions cellular aggregates and biofilms are formed, what their influence in strain resistance to several stresses are and, their role as virulence factors. With this aim, a basic artificial sputum medium (ASM) was developed to grow *P. aeruginosa* (Sriramulu et al. 2005). As the name suggests, this medium simulates the CF natural lung habitat, containing components that are thought to be present in CF lungs *(e.g.,* mucin, DNA, surfactant, salt ions, iron and amino acids) (Ghani and Soothill 1997). Mucin is the major energy source of the medium, as its absence leads to lower growth of *P. aeruginosa* (Sriramulu et al. 2005). Within this medium, some strains of *P. aeruginosa* are able to form cellular aggregates, or "visible clumps" as mentioned by Sriramulu *et al.*, demonstrating its potential behaviour when growing inside CF patient's lungs.

In *P. aeruginosa*, cellular aggregates are formed during the process of biofilms establishment, which formation is led by EPS production (Petrova et al. 2012) and by the repression of RetS, which usually interacts with GacS sensor protein preventing the activation of GacAS pathway and repressing biofilm formation (Goodman et al. 2009; Workentine et al. 2010). The colonization of epithelial cells by *P. aeruginosa* occurs in two steps: first, cells proliferate and adhere to the epithelial cells, where cellular aggregates formation starts, and biofilms are established; after this, in step two, individual

bacteria belonging to the aggregates start to disperse, allowing proliferation and new colonization (Engman et al. 2017).

Besides EPS, conventional biofilms are composed by other molecules such as extracellular DNA, amino acids, salt and low iron concentrations (Sriramulu et al. 2005) which are also present in ASM medium. Each of these components present a function in biofilms dynamics. The presence of amino acids helps to define the tightness of aggregates, once its absence leads to the formation of smaller aggregates and an increased number of planktonic cells (free cells) (Sriramulu et al. 2005). Extracellular DNA is responsible for mature biofilms stabilization and for cell-to-cell interconnecting (Allesen-Holm et al. 2006). Its release occurs via lysis of a small subpopulation of cells or via lysis of small vesicles containing DNA which are released from bacteria (Allesen-Holm et al. 2006). In young biofilms, cells are held together by extracellular DNA; on the other hand, older biofilms cells are held together not only by extracellular DNA, but mostly by other compounds, including EPS. Such conclusions are possible because, according to Whitchurch *et al.* a DNase treatment lead to young biofilms dissolution whereas older biofilms were only partially affected. These facts were justified by Allesen-Holm et al. suggesting that at late-log phase of growth the amount of DNA released is higher than in the initial and mid-log phase of growth. The fact that extracellular DNA is mainly released in late-log phase of growth suggests that quorum-sensing might have a role in DNA release during biofilm and cellular aggregates formation (Allesen-Holm et al. 2006). The construction of *P. aeruginosa lasIrhI* mutants showed that they were not able to release an high amount of DNA in the late-log phase of growth, however the supplementation of the medium with signal molecules restored the accumulation of extracellular DNA during late-phase (Allesen-Holm et al. 2006). Although the signal molecules are present during all growth phases, the release of high amounts of DNA only occurs during late phases. This suggests that the quorum sensing-regulated DNA release process may also be regulated by other systems than *las* and *rhI* (Medina, Juárez, and Soberón-Chávez 2003).

Biofilms and, consequently, cellular aggregates formation are mainly regulated by quorum-sensing. This mechanism enables bacteria to control its cell population density through extracellular signalling molecules accumulation (Davies et al. 1998). Three quorum-sensing systems are responsible for controlling the expression of several virulence factors in *P. aeruginosa*. These systems are *lasRI, rhIRI* and *Pseudomonas* quinolone signal (PQS). The *rhIRI* system is controlled by the *lasRI* system (Latifi et al. 1995; Passador et al. 1993). In its turn, PQS system is also controlled by *lasRI* system (Pesci et al. 1999). The relation between extracellular DNA release and quorum-sensing systems is visible in PQS system. It was observed that in strains with a much more pronounced lysis, PQS was overproduced (Argenio et al. 2002). PQS overproduction leads to cell lysis which, consequently, leads to extracellular DNA release. With this, biofilms development increases (Argenio et al. 2002).

1.1. Cystic Fibrosis

Cystic fibrosis is an autosomal recessive disease. First, CF was described as a defective chloride permeability of plasma membranes in the lung disease, leading to respiratory failure. Later, the gene responsible for the disease was identified and its product was named CFTR. CFTR structure placed it in the ATP-biding cassette (ABC) gene family. CFTR protein contains two ATP-hydrolysis domains (nucleotide-biding domains) and, 12 membrane-spanning alpha helixes (Figure 1).

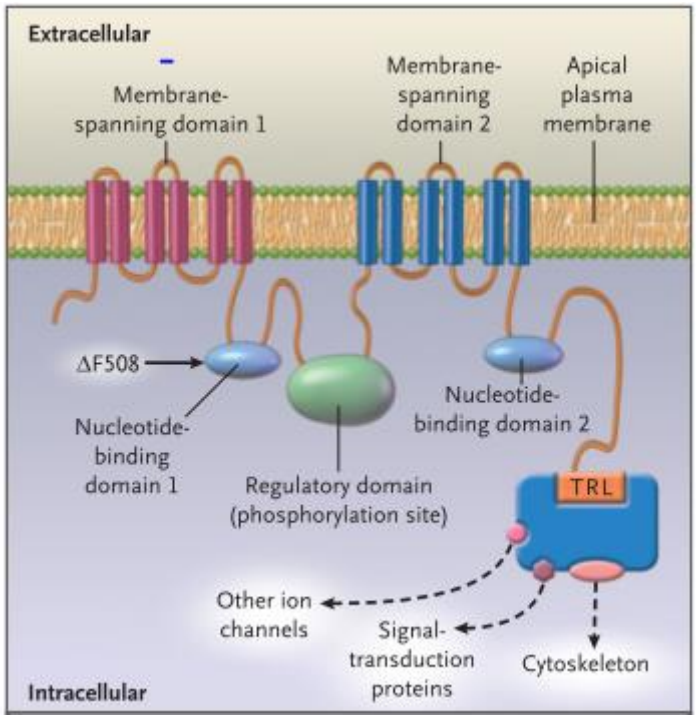

Figure 1 CFTR structure. Its activations rely on phosphorylation through protein kinase A, but also other kinases. The two nucleotide-domains regulate the channel gating. The six membrane-spanning alpha helixes form a chloride-conductance pore (retrieved from Paranjape and Mogayzel Jr. 2014)

Besides chloride transport, CFTR has other functions. Namely, it down-regulates transepithelial sodium transport, the epithelial sodium channel, regulates calcium-activated chloride channels and potassium channels, it also serves important functions in exocytosis and the formation of molecular complexes in the plasma membrane (Paranjape and Mogayzel Jr. 2014). In CF patients the deletion of *cftr* gene influences the expression of important proteins in inflammatory responses, ion transport and cell signalling, suggesting that CFTR functions go beyond chloride permeability.

In CF patients, exocrine and submucosal glands are obstructed with thick mucosal secretions, being this the major contributor to morbidity and mortality in these patients (Paranjape and Mogayzel Jr. 2014). Blockage of the airways by thick, viscous, neutrophil-dominated mucopurulent debris is one of pathological hallmarks of the disease.

As previously mentioned, CF patients are colonized by specific pathogens such as *P. aeruginosa, Burkholderia cepacia* complex bacteria*, Staphylococcus aureus,* and *Haemophilus influenzae*, among others. These species become well established within the patient airways, causing chronic infections. These chronic infections turn the bacteria difficult to eradicate. Taking *P. aeruginosa* as an example, this bacteria is capable of adapting to the lung microenvironment in CF patients by producing biofilms, cellular aggregates, and a capsular polysaccharide that inhibits antibiotic penetration and confers a mucoid phenotype (Wyckoff et al. 2002; Whiteley et al. 2001). Before chronic infection establishment, inflammatory processes are a major concern and are the cause of respiratory insufficiency in CF patients (Paranjape and Mogayzel Jr. 2014). Inflammatory mediators, such as neutrophil elastase and bacterial lipopolysaccharide, are recognized by toll-like receptors, which mediate inflammatory effects by activating the transcription factor-kB, which controls a molecular pathway that is responsible for the production of inflammatory proteins (Sagel et al. 2002).

The absence of normal CFTR activity in CF patients, does not only affect their respiratory capacity but, also causes the obstruction of other organs (Paranjape and Mogayzel Jr. 2014). It can cause intestinal obstruction, infertility in man, pancreatic insufficiency and, hepatic problems that could lead to cirrhosis. Defects in ion transport and salt homeostasis are related to organ damage in CF patients (Paranjape and Mogayzel Jr. 2014). The absence of a functioning CFTR in these patients limits the amount of salt that can be regained since, the reabsorption of chloride is restricted. Because of similar reasons, sodium is poorly absorbed, causing a salty sweat on the skin surface. This means that, people without the disease are capable of absorb chloride before the emergence of sweat to the skin surface (Figure 2) (Paranjape and Mogayzel Jr. 2014).

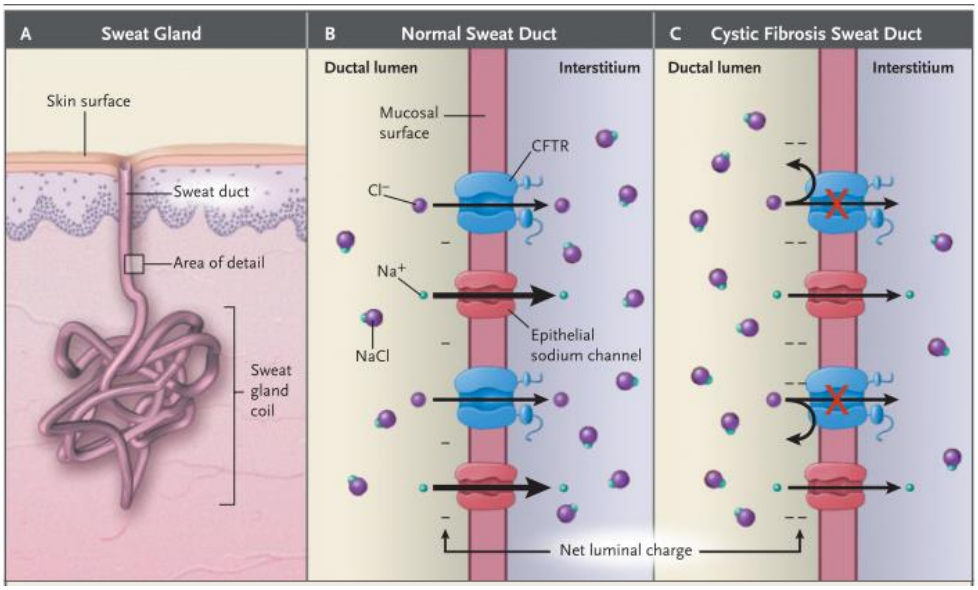

Figure 2 Differences between a person without CF (B) and a person with CF (C), it is possible to understand that in a CF patient the absorption of chloride does not occur. Image A represents a normal sweat gland**.**

The signs and symptoms that can manifest helping to diagnose the disease vary with age, however there are some symptoms that occur in all ages. The general symptoms are a family history of cystic

fibrosis, a salty-tasting skin, clubbing of fingers and toes, a cough with sputum production, presence of *P. aeruginosa* in airways secretions and hypochloraemic metabolic alkalosis. Other symptoms only occur in certain ages; at neonatal the symptoms are meconium ileus, protracted jaundice, abdominal or scrotal calcifications and intestinal atresia. During infancy the symptoms are the presence of persistent infiltrates on chest radiographs, failure to thrive, anasarca or hypoproteinaemia, chronic diarrhoea, abdominal distention, cholestasis, pneumonia caused by *S. aureus*, and vitamin A and E deficiency. At childhood the CF symptoms are chronic pansinusitis or nasal polyposis, steatorrhoea, rectal prolapse, distal intestinal obstruction syndrome, chronic pancreatitis and liver disease. At last, during adolescence and adulthood the main symptoms are allergic bronchopulmonary aspergillosis, chronic pansinusitis, bronchiectasis, haemoptysis, recurrent pancreatitis, portal hypertension, delayed puberty and azoospermia in men's (O'Sullivan and Freedman 2009).

The treatments administrated to patients depends on the severity of the disease. Most of treatments are oral or intravenous antibiotics (O'Sullivan and Freedman 2009). The most used antibiotics are dornase alfa, tobramycin to patients with severe or moderate symptoms, colistine, hypertonic saline, ibuprofen, macrolide antibiotics such as azithromycin, are also used.

The prevalence of CF varies from country to country, and with ethnic background. Northern European descenders have greater recurrence, occurring in approximately 1 in 3000 births (O'Sullivan and Freedman 2009). The lower prevalence is in Africa and Asia, being the frequency of 1 in 350000.

1.2. Genetic and environmental factors affecting cellular aggregate and biofilm formation in bacteria

1.2.1. In *Mycobacterium abscessus*

Cellular aggregates development can increase bacteria virulence, especially when these organisms are pathogenic to humans. An example of this is *Mycobacterium abscessus*, in which cellular aggregates formation leads to an increased virulence. Like *P. aeruginosa* and *B. cepacia* complex bacteria, *M. abscessus* is a serious human pathogenic species that causes chronic pulmonary infection in patients with respiratory diseases, such as cystic fibrosis (Brambilla et al. 2016). This phenotypic change is thought to be associated to a response to Toll like receptor-2 (TLR-2) ligands expressed on the bacterial cell surface (Brambilla et al. 2016). To confirm that aggregates increase strain virulence, assays with infected macrophages were performed (Brambilla et al. 2016). Normal macrophages were infected with two different *M. abscessus* morphotypes, one in which cells were aggregated, and the other in which cells were isolated bacilli (non-aggregated cells). Both morphotypes infected macrophages in similar proportions (between 50 and 60%), which means that both aggregates and isolated bacilli were observed inside macrophages vesicles (Figure 3).

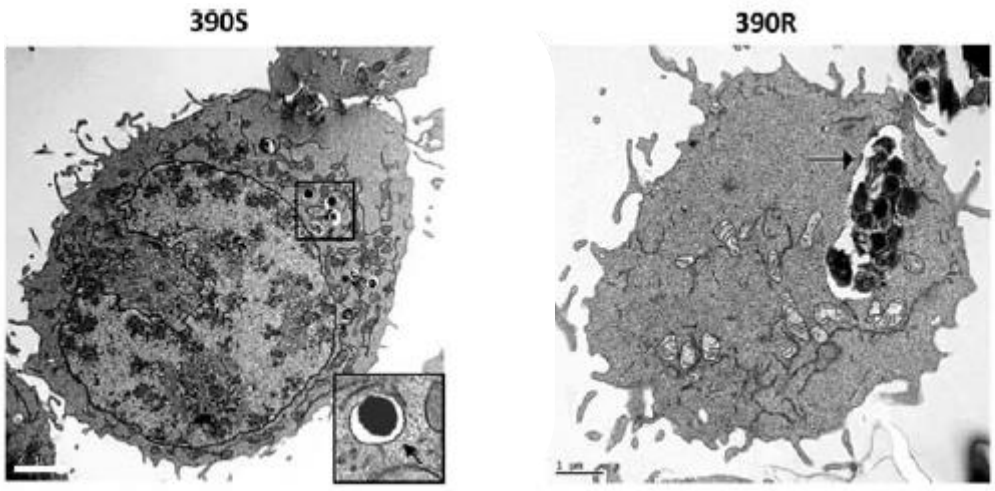

Figure 3 Macrophages infected with *M. abscessus* cells. 390S corresponds to a macrophage infected with isolated bacilli, and 390R corresponds to a macrophage infected with aggregated cells (retrieved from Brambilla et al. 2016).

Although both morphotypes were capable of infecting macrophages, different effects were observed due to their presence. Macrophages infected with isolated bacilli showed a similar appearance to the uninfected macrophages, whereas macrophages infected with aggregated cells were damaged (Figure 4) (Brambilla et al. 2016).

This experiment shows that macrophages can phagocytose both individual cells and *M. abscessus* aggregates (Brambilla et al. 2016). Aggregates are able to grow inside phagocytic vesicles, which eventually kill macrophages, which subsequently liberate large aggregates into extracellular space (Brambilla et al. 2016).

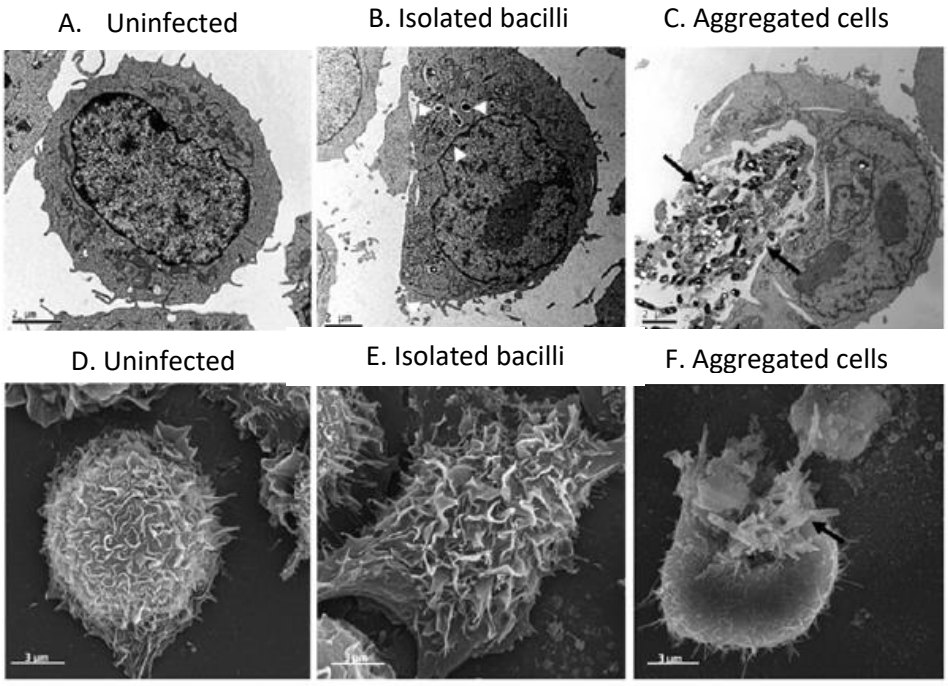

Figure 4 Visible effects in macrophages due to infection with *M. abscessus*. (A and D) Uninfected macrophage. (B and E) Macrophage infected with isolated bacilli. (C and F) Macrophage infected with aggregated cells. Images A, B and C were obtained through Transmission Electron Microscopy (TEM). Images D, E and F were obtained through Scanning Electronic Microscopy (SEM) (retrieved from Brambilla et al. 2016).

1.2.2. In *Pseudomonas aeruginosa*

P. aeruginosa is a Gram-negative bacterium that grows in soil, marine environments, plant and animal tissues (Hardalo and Edberg 1997). *P. aeruginosa* is also known as an important opportunistic human pathogen. As previously cited, this species can produce cellular aggregates and biofilms, leading to chronic lung infections. Because of these structures, *P. aeruginosa* presents increased resistance to administrated treatments.

In *P. aeruginosa,* cellular aggregates (also named microcolonies) and biofilm formation is regulated by a two-component factor, MifR. A transcriptome analysis demonstrated that genes MifR-dependent encode proteins involved in metabolic, biosynthetic, energetic processes and membrane proteins including those responsible for small molecules transport (Figure 5) (Petrova et al. 2012).

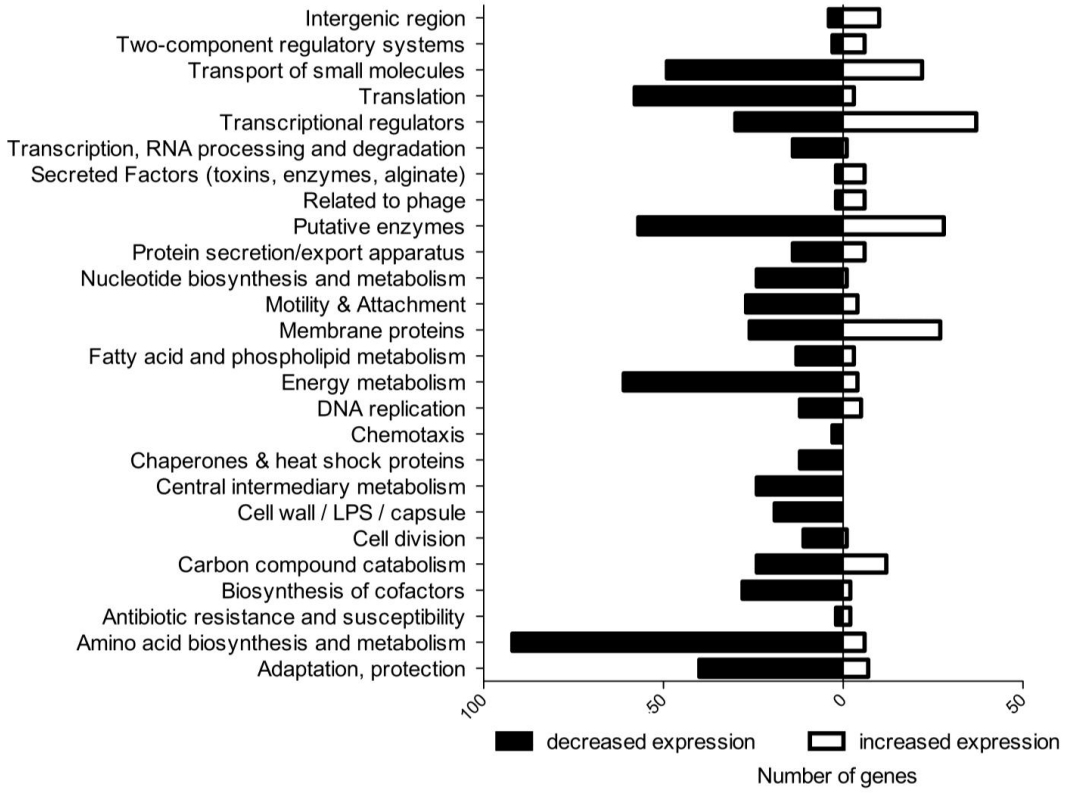

Figure 5 Genes MifR-dependent and its level of expression when compared with Δ*mifR P. aeruginosa* (retrieved from Petrova et al. 2012).

The proteins with reduced expression in the mutant strain (Δ*mifR*) biofilms are associated with anaerobic growth. In this group are included aconitase (AcnA), stress response proteins (UspK and UspN) and an outer membrane protein (OprE) (Petrova et al. 2012). The increased concentration of these proteins during cellular aggregates formation is related to anaerobic growth (6, 7, 8, 9). With these findings it can be considered that cellular aggregates formation in *Pseudomonas aeruginosa* it is not only fully dependent on a two component regulator, MifR, in which overexpression of *mifR* is responsible for an increase of cellular aggregates, but also correlated with oxygen-limiting conditions (Petrova et al. 2012). However, *P. aeruginosa* is unable of growing under strictly anaerobic conditions (Petrova et al. 2012). Besides of favouring aggregation, oxygen-limiting conditions promotes resistance against antibiotics such as ciprofloxacin and tobramycin in *P. aeruginosa* (Borriello et al. 2004). This may explain why antibiotic therapy fails to control infection associated with *P. aeruginosa.* This stress condition, as many other described below, can help to explain how cellular aggregates develop and, in which way these aggregates may influence the resistance to therapies presented by *P. aeruginosa,* and other microorganisms*.*

1.2.2.1. Role of pyruvate and iron concentrations

The expression of genes responsible for aggregates formation is, usually, triggered by extra and intracellular conditions. It is known that pyruvate (Petrova et al. 2012) and iron (Banin, Vasil, and Greenberg 2005) concentrations present in extracellular environment are important for cellular

aggregates development. Growth in the presence of pyruvate is possible due to UspK expression, as this protein plays a role in fermentative growth on medium containing this substrate (Schreiber et al. 2006). This fact leads to the thought that UspK protein is require to cellular aggregates formation since it promotes the process in conditions that triggers fermentative metabolism (Petrova et al. 2012). Addition of pyruvate to the growth medium (extracellular stress) promotes aggregates formation but, intracellular pyruvate concentrations may also contribute to the process, since *P. aeruginosa* is able to release pyruvate to the extracellular environment and metabolize it during stationary phase. It is important to notice that the effect of pyruvate on cellular aggregates development continues to be dependent on oxygen-limiting conditions (Petrova et al. 2012). With the measurement of $NADH/NAD^+$ ratio inside the cells after the addition of pyruvate, it was possible to understand that pyruvate is used as redox balancing, which is required to enable cellular aggregates formation (Petrova et al. 2012).

Low iron availability in medium (5 µM $FeCl_3$), also promotes cellular aggregates formation in *P. aeruginosa* (Yang et al. 2017). With an opposite effect, an increasing of iron concentrations (100 µM $FeCl_3$) promotes the decreasing of cell aggregates and biofilm formation (Figure 6) and, as a consequence, occurs a decrease in subpopulations with increased tolerance against antimicrobial compounds (Yang et al. 2017). Besides these facts, high iron concentration promotes the development of unstructured biofilms, with less spatially organization. In order to have an influence in biofilm formation, iron needs to be transported into the cell (an uptake needs to occur). For this purpose, *P. aeruginosa* has two main iron acquisition systems, pyoverdine system (high-affinity) and pyochelin system (low-affinity), which binds extracellular iron (Fe^{3+}) and transport it into the cell (Banin et al 2005). In the absence of the uptake system, thin and flat biofilms are. Contrary to this, the presence of an uptake system leads to aggregates formation, mature mushroom-like structures under the same conditions described above (Banin et al 2005). Besides extracellular iron, intracellular iron concentration is also responsible for aggregates development. Intracellular iron concentration is regulated by an iron-dependent transcription repressor, Fur, which also controls crucial genes in biofilm and aggregates formation (Banin et al 2005).

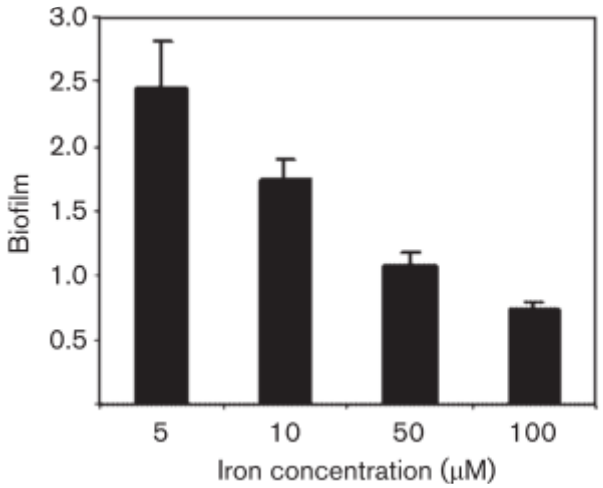

Figure 6 Relative amounts of biofilm according with different iron concentrations. It is possible to understand the existence of a direct proportion between iron concentrations and biofilm formation. (retrieved from Yang et al. 2017).

As mentioned before, low iron concentrations promote biofilm and aggregates formation. However, this regulation does not occur in a direct process. The formation of cellular aggregates and biofilms, occurs via up-regulation of the *pqs* genes (quorum-sensing system) and formation of extracellular DNA (Yang et al. 2017). As mentioned before, high amounts of DNA release occur during late-phases of growth. When analysing late-phase cells is possible to observe large cellular aggregates among planktonic cells. Such aggregates were not observed in *lasIrhII* mutants (regulators of PQS system). This suggests that extracellular DNA release is a contributing factor to cellular aggregates development (Allesen-Holm et al. 2006).

1.2.2.2. Role of biofilm constituents

Other biofilm components are also promoters of cellular aggregates formation and, an influence in their morphology. An example are amino acids. These molecules are required for the formation of tight cellular aggregates (Sriramulu et al. 2005).

The formation of cellular aggregates can also be promoted by virulence factors such as Trp and other structural components such as LPS (lipopolysaccharides) and outer-membrane protein OprF (Sriramulu et al. 2005). Trp is a type IV pili responsible for adhesion, autoaggregation and biofilm formation in Gram-positive and Gram-negative bacteria (Engman et al. 2017).

1.2.2.3. Role of temperature

Temperature plays a role in cellular aggregation. In the case of *P. aeruginosa* higher temperatures tend to decrease autoaggregation capacity. According to Argenio *et al.*, *P. aeruginosa* insertion mutant *wspF10* (which present a high autoaggregative ability) when grown in LB, has a diffuse turbidity at 42ºC, while at 23ºC only presents a pellicle with low planktonic cells. Other spontaneous *P. aeruginosa* mutants exhibit similar phenotypes (Argenio et al. 2002).

1.2.2.4. Role of magnesium concentrations

Magnesium present in the extracellular environment is sequestered by extracellular DNA, being this a chelator of divalent cations. Mg^{2+} limitation represses *retS* expression (a biofilm repressor), leading to increase aggregation, EPS production and biofilm formation (Mulcahy and Lewenza 2011). The presence of Mg^{2+} in medium is sensed by the two-component system, PhoPQ, which in turn represses *retS* promoting cellular aggregates development (Mulcahy and Lewenza 2011). To confirm that limiting Mg^{2+} concentrations are responsible for promoting cellular aggregate development, Mulcahy *et al.* monitored EPS production under high and low magnesium concentrations by planktonic and aggregated cells. Under Mg^{2+} limiting conditions higher concentrations of EPS were produced, comparing with high Mg^{2+} conditions (Figure 7) (Mulcahy and Lewenza 2011). As expected, the *retS* mutant exhibited elevated EPS production.

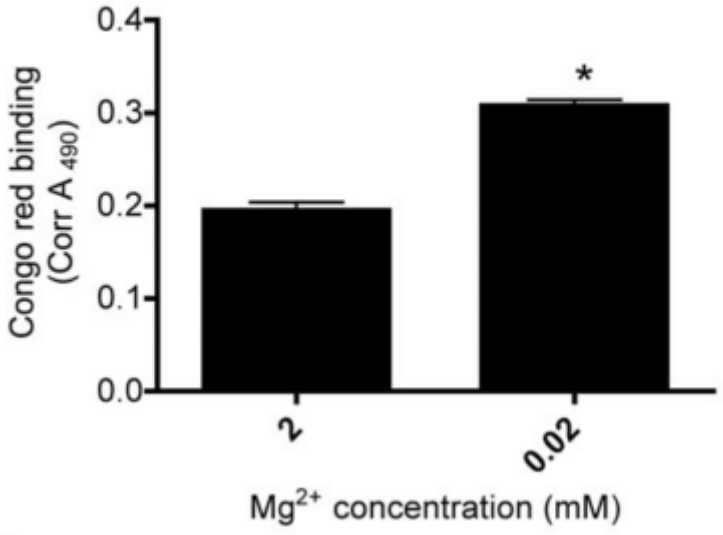

Figure 7 EPS production of *P. aeruginosa* under 0.02 and 2 mM Mg^{2+}. The EPS production was measured using the congo red assay (retrieved from Mulcahy and Lewenza 2011).

With these results, it is possible to conclude that Mg^{2+} limiting conditions are responsible for increased aggregation, EPS production and an hyperbiofilm phenotype through PhoP-mediated repression of *retS* expression (Mulcahy and Lewenza 2011).

1.2.3. In *Azospirillum brasilense*

In the species *Azospirillum brasilense*, many factors are involved in the cellular aggregation process, such as extracellular stress and metabolic products produced by aggregated cells. In aggregated cells high amounts of poly-*β*-hydroxybutyrate (PHB) (Burdman et al. 1998) and a thick layer of EPSs were observed.

1.2.3.1. Role of oxygen and nitrogen concentrations

The oxygen gradient in the culture medium has a key role in cellular aggregation. However, the oxygen concentration needed to trigger aggregates development is not equal to all species capable of producing such structures. As mentioned before, in *P. aeruginosa* cellular aggregation is triggered by low oxygen concentration (Petrova et al. 2012) but, contrary to this species *Azospirillum brasilense* only develops cellular aggregates in the presence of high oxygen concentration in its environment (Bible et al. 2015). In the case of *A. brasilense* cellular aggregates formation is caused by a reduced action of Che1, a chemotaxis signalling pathway. Che1 is responsible for controlling the swimming speed of *A. brasilense* during chemotaxis, more specifically, in oxygen gradients (Bible et al. 2015). Mutant strains lacking CheY1 regulator, present a much higher aggregation rate than its wild-type when under high oxygen concentrations (Bible et al. 2015). According to Bible *et al.* two mutants were created with the aim of studying the effect of high oxygen concentration in aggregates formation. The two deletion mutants were BS106 (Δ*cheB1* Δ*cheR1*) which does not produce any aggregates and, AB104 (Δ*cheY1*) which overproduces aggregates when comparing with the wild-type strain. When comparing mutants, it was possible to understand that the up- and downregulation patterns were different between them. This indicates that each mutant strain has its unique physiological response to the stressful environment (Bible et al. 2015). The differences analysed between the three strains after the stress was applied, indicates the physiological changes that occur due to cellular aggregation under increased oxygen concentrations. Comparing the wild-type strain with the over productive strain, it was observed that key enzymes in amino acid biosynthesis are overexpressed in AB104 mutant (Bible et al. 2015). Presenting an opposite expression level, a putative urease and an aspartokinase were downregulated in the same strain. This increase in amino acid biosynthesis due to elevated oxygen levels coincide with a decreased expression of proteins involved in amino acid utilization during catabolism. Such fact is in agreement with aggregated cells adopting a metabolism which aims a behaviour of amino acids conservation (Bible et al. 2015).

Along with high oxygen concentrations, nitrogen limitation promotes aggregates development, under the same Che1 regulation (Bible et al. 2015). A nitrogen limitation is faced as a nutrient-starvation stress. A nutrient-starvation stress leads to a dramatic change in cell metabolism. When subject to a limited nitrogen concentration, AB104 overexpressed proteins were involved in the accumulation of carbon storage materials such as glycogen, and acetyl coenzyme A (CoA) synthetase. The metabolic changes are not only represented by overexpression of proteins. These changes also involve a reduced expression of several proteins involved in glycolysis and pentose phosphate pathway, which is in agreement with the overexpression of proteins responsible for the accumulation of carbon storage materials (Bible et al. 2015). Cellular aggregation is a nutrient-scavenging strategy, as metabolism modification also cover up- and downregulation of several transporters. By this, increased aggregation cell's metabolism modifications also increase (Bible et al. 2015). By the adoption of a nutrient-scavenging behaviour, cells increase their carbon storage and

amino-acid conservation, preparing themselves to further nutritional stresses that may occur during their growth.

As mentioned before, some authors distinguish clumps from flocculation when studying cellular aggregate structures. In the case of Bible *et al.* this distinction is made. Clumps formation is always obligatory to floccus formation. In the case of *A. brasilense* both behaviours occur under conditions of metabolism imbalance, elevated oxygen concentrations and, limitations in the availability of a nitrogen source. Therefore, for flocculation to occur, elevated oxygen levels and nitrogen-limiting (fixed nitrogen, in the form of ammonium) concentrations need to exist in growth medium (Bible et al. 2015). During flocculation process occurs an increase of EPS production within the cell, which represents a profound reorganization of cells physiology (Bible et al. 2015). To confirm the importance of the presence of nitrogen in growth medium, mutants defective in genes involved in nitrogen sensing metabolism (*amtB*, *ntrC*, *glnB* and *glnZ*) were tested (Bible et al. 2015). The *amtB* and *ntrC* mutants had a reduced clumping and flocculation phenotype, while *glnB* and *glnZ* mutants demonstrated reduced clumping and were severely affected in flocculation (Bible et al. 2015). By this, it is possible to conclude that low nitrogen levels are a trigger signal for flocculation. Nitrogen and oxygen concentration work together as trigger signal of clumping and flocculation. Aggregated cells (clumping and flocculating cells) are protected from continuous oxygen stress, as these cells are able to maintain a microaerophilic intracellular environment, which is compatible with nitrogenase expression, an oxygen-sensitive enzyme. This enzyme is responsible for nitrogen fixation, suggesting that intracellular conditions during aggregates development are sufficient to induce nitrogenase expression (Bible et al. 2015). The development of such structures enables *A. brasilense* to adjust its metabolism as a response to the imposed stress, by scavenging carbon and nitrogen nutrients (Bible et al. 2015).

Additionally, for cellular aggregates to develop the medium needs to have a high C:N ratio. *A. brasilense* uses as a carbon source fructose, and as a nitrogen source ammonium chloride (NH_4Cl). However, other carbon sources such as arabinose, galactose and glycerol can be used, being the results similar to the one's obtained with fructose as a carbon source (Burdman et al. 1998). On the other hand, the use of malate and succinate led to a non-production of aggregates. These results may suggest that drastic changes in the media pH may be important in cellular aggregates formation.

1.2.3.2. Role of temperature and pH levels

Stresses such as medium pH was analysed by Burman et al.. At all pH values, aggregates were stable and remained intact for several days. However, in more acidic pH, was observed an increased aggregation. According to Burdman et al., this fact may be due to negative ionized groups that are neutralized and by this, the repulsive forces between bacteria decreased, promoting aggregation.

1.2.4. In *Burkholderia multivorans*

Although there is a lot of knowledge on the formation of conventional biofilms by the *Burkholderia cepacia* complex bacteria, only one publication reports planktonic cellular aggregates formation (Silva et al., 2017). These authors have shown that both environmental and clinical isolates from several Bcc species are able to form aggregates in salts medium containing several sugars/sugar alcohols such as fructose, glucose or mannitol. In particular, they have found that deleting from the genome of *B. multivorans* ATCC 17616, the transcriptional regulator LdhR which controls de expression of lactate dehydrogenase enzyme LdhA, strongly decreased the size of the formed aggregates (Figure 8). The most likely explanation is that lactate dehydrogenase is needed inside the aggregates where oxygen levels are low and cells might need to ferment pyruvate into lactate for energy purposes.

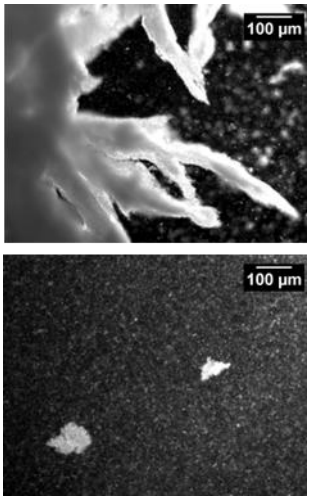

Figure 8 Images of the planktonic cellular aggregates that sediment after 5 minutes static incubation of cultures grown for 72 hours under constant agitation in medium containing 2% D-mannitol. The wild-type strain *B. multivorans* ATCC 17616 (upper panel) and *ΔldhR* mutant (lower panel) are shown (adapted from Silva et al. 2017).

1.3. Objectives of this study

This work is within a major project aiming to elucidate some adaptations involved in the transition undertaken by *Burkholderia cepacia* complex bacteria to form chronic infections in the CF lung. Despite our knowledge on some of the phenotypic transitions occurring during Bcc lung colonization, not many studies evaluating cellular aggregates formation by *Burkholderia* have been reported. Cellular aggregation in these microorganisms is very likely, a response to stress conditions, in which cells become more protected from external aggressions such as oxidative stress, antimicrobial therapies, and phagocytosis by the immune system. If we could prevent the formation of these aggregates, perhaps it would improve the chances of bacterial eradication by the immune system and/or antimicrobial therapy. The specific goals are:

- Evaluate if cellular aggregation is conserved throughout chronic infection of CF lung by longitudinal series of *Burkholderia multivorans;*
- Identify environmental conditions triggering aggregation;
- Confirm whether the enzyme lactate dehydrogenase is a player in this process, similarly to previous findings in another *B. multivorans* strain and in *P. aeruginosa*;
- Evolve the cellular aggregation phenotype under laboratory conditions in order to find key genetic players.

2. Materials and methods

2.1. Bacterial strains and growth conditions

Bacterial strains used during the studies are *Burkholderia multivorans* isolates recovered from Cystic Fibrosis patients (Table 1). During the studies, all strains were kept at -80ºC in 30% glycerol. When in use, strains were kept in Luria-Bertani medium (LB medium) and, mutant strains were kept in LB medium supplemented with respective antibiotics, according with the vectors used during their construction. While in study, the isolates plates were maintained at 4ºC, after growing at 37ºC in its respective media.

In addition to the studied isolates, a mutant *B. multivorans* Δ*ldhA* was constructed during this project.

To test the presence of cellular aggregates, the different isolates were inoculated for 72h, at 37ºC and 180 rpm in S medium (12.5 g Na_2HPO_4, 3 g KH_2SO_4, 1 g NaCl, 1 g casaminoacids, 1 g yeast extract, 0.2 g/L Mg^{2+}, 0.001 g/L Fe^{2+} and 0.01 g/L Ca^{2+}) supplemented with 2% of Mannitol (SM medium).

After the determination of the minimal inhibitory concentration of ciprofloxacin antibiotic, the isolates were incubated for 48h at 37ºC and 180 rpm in SM medium supplemented with the chosen antibiotic concentration.

Table 1 Date of isolation and ID of the several isolates belonging to the nine patients studied.

Isolate	ID	Date of isolation	Isolate	ID	Date of isolation	Isolate	ID	Date of isolation	Isolate	ID	Date of isolation
P0213-1	VC7495	13/2/1996	P0148-4	VC4956	10/11/1992	P0205-2	VC7102	26/05/1995	P0205-21	VC16559	28/02/2013
P0213-2	VC7704	4/6/1996	P0148-5	VC5420	29/08/1993	P0205-3	VC7731	14/06/1996	P0205-22	VC16929	27/10/2013
P0213-3	VC7804	13/8/1996	P0148-6	VC5421	29/08/1993	P0205-4	VC7732	14/06/1996	P0205-23	VC17637	21/03/2015
P0213-4	VC8896	6/5/1998	P0148-7	VC6274	20/05/1994	P0205-5	VC8270	6/06/1997	P0339-1	VC6880	21/02/1995
P0213-5	VC9452	20/1/1999	P0148-8	VC6275	20/05/1994	P0205-6	VC8999	20/06/1998	P0339-2	VC9604	4/05/1999
P0213-6	VC10037	18/1/2000	P0148-9	VC7067	5/05/1995	P0205-7	VC10371	23/09/2000	P0339-3	VC10336	24/08/2000
P0213-7	VC10458	7/11/2000	P0148-10	VC7515	23/02/1996	P0205-8	VC11265	29/03/2002	P0339-4	VC11038	6/11/2001
P0213-8	VC11002	23/10/2001	P0148-11	VC7614	12/04/1996	P0205-9	VC13059	31/10/2005	P0339-5	VC11508	5/09/2002
P0213-9	VC11446	23/7/2002	P0342-1	VC12539	23/09/2004	P0205-10	VC13400	1/06/2006	P0339-6	VC12155	20/11/2003
P0213-10	VC12063	26/9/2004	P0342-2	VC12721	31/01/2005	P0205-11	VC13401	1/06/2006	P0280-1	VC6882	21/02/1995
P0213-11	VC12556	30/9/2004	P0342-3	VC13492	15/09/2006	P0205-12	VC13534	9/11/2006	P0280-2	VC7835	4/09/1996
P0213-12	VC13750	11/4/2007	P0342-4	VC13732	28/03/2007	P0205-13	VC14024	27/10/2007	P0280-3	VC9600	4/05/1999
P0213-13	VC13748	11/4/2007	P0342-5	VC14645	2/02/2009	P0205-14	VC14765	7/05/2009	P0280-4	VC10360	15/09/2000
P0213-14	VC13833	20/6/2007	P0342-6	VC15079	13/01/2010	P0205-15	VC15201	19/04/2010	P0280-5	VC11148	10/01/2002
P0213-15	VC13834	20/6/2007	P0342-7	VC15604	18/05/2011	P0205-16	VC15656	20/06/2011	P0280-6	VC11694	10/01/2003
P0213-16	VC15071	11/1/2010	P0342-8	VC15605	18/05/2011	P0205-17	VC15765	23/09/2011	P0280-7	VC11966	27/06/2003
P0148-1	VC3161	21/02/1989	P0342-9	VC15918	17/12/2011	P0205-18	VC15766	23/09/2011	P0280-8	VC11967	27/06/2003
P0148-2	VC4502	26/11/1991	P0342-10	VC16176	20/06/2012	P0250-19	VC16144	31/05/2012	P0280-9	VC12602	3/11/2004
P0148-3	VC4503	16/11/1991	P0205-1	VC5602	30/11/1993	P0205-20	VC16557	28/02/2013	P0280-10	VC12711	18/01/2005

P0280-11	VC12892	2/06/2005	P0426-7	VC11369	24/05/2002	P0426-21	VC17390	22/09/2014	P0686-1	VC12675	15/12/2004
P0280-12	VC13437	28/06/2006	P0426-8	VC11982	17/07/2003	P0431-1	VC9159	22/09/1998	P0686-2	VC12676	15/12/2004
P0280-13	VC13686	25/02/2007	P0426-9	VC12458	22/07/2004	P0431-2	VC9419	12/01/1999	P0686-3	VC12677	15/12/2004
P0280-14	VC13703	28/02/2007	P0426-10	VC13030	22/09/2005	P0431-3	VC9663	1/06/1999	P0686-4	VC12678	15/12/2004
P0280-15	VC13756	17/04/2007	P0426-11	VC13616	12/01/2007	P0431-4	VC9937	9/11/1999	P0686-5	VC12735	10/02/2005
P0280-16	VC13757	17/04/2007	P0426-12	VC13617	12/01/2007	P0431-5	VC10206	6/06/2000	P0686-6	VC13239	2/02/2006
P0280-17	VC14135	13/01/2008	P0426-13	VC13777	2/05/2007	P0431-6	VC10207	6/06/2000	P0686-7	VC13240	21/02/2006
P0280-18	VC14224	10/03/2008	P0426-14	VC13778	2/05/2007	P0431-7	VC10812	26/06/2001	P0686-8	VC13637	24/01/2007
P0426-1	VC8086	11/02/1997	P0426-15	VC14363	6/07/2008	P0431-8	VC11330	14/05/2002	P0686-9	VC14586	5/12/2008
P0426-2	VC8136	17/03/1997	P0426-16	VC14863	11/08/2009	P0431-9	VC12100	21/10/2003	P0686-10	VC15535	31/03/2011
P0426-3	VC8585	20/01/1998	P0426-17	VC15667	23/06/2011	P0431-10	VC12273	25/02/2004	P0686-11	VC15917	15/12/2011
P0426-4	VC9177	25/09/1998	P0426-18	VC15867	17/11/2011	P0431-11	VC12274	25/02/2004			
P0426-5	VC9783	12/08/1999	P0426-19	VC16979	4/12/2013	P0431-12	VC12720	30/01/2005			
P0426-6	VC10411	12/10/2000	P0426-20	VC17389	22/09/2014	P0431-13	VC13473	1/08/2006			

2.2. DNA extraction

For both genomic and plasmid DNA extraction kits were used. QIAGEN® DNeasy® Blood and Tissue kit was used to perform genomic DNA extraction. The protocol followed during the extraction was according with the manufactures' instructions. ZR Plasmid Miniprep™ kit from ZYMO RESEARCH® was used to perform the extraction of plasmid DNA. The protocol followed during the procedure was the one provided by this specific kit.

2.3. *B. multivorans* Δ*ldhA* mutant construction

To obtain the *B. multivorans* Δ*ldhA* mutant two different vectors were used (Figure 9). In a first approach the two flanking regions of *ldhA* gene belonging to *B. multivorans* isolate P0213-1 were amplified by PCR. For the amplification process, genomic DNA was extracted and the following primers sets, including restriction enzymes, were used for each region. For the the upstream region the primers were *LdhR*_Fw 5'- GGGGTACCCCGGGCCAAAAATACGCAAG – 3', and

*LdhR*_Rev 5' – GCTCTAGACGGCTGCTGAACAGGATCAC – 3'. For downstream region the primers were *Bmul_25591*_Fw 5' – GCTCTAGATATCGTTCGCCGACCTTC – 3' and *Bmul_2559*_Rev 5' – GGAGCTCGCGATAGCGGCGATTCTA – 3'. After PCR procedure, purification of the resulting DNA was performed using DNA Clean and Concentrator™ kit from ZYMO RESEARCH®. After DNA purification both amplified fragments and pBCSK⁺ vector was doubled digested by the enzymes described in Table 2. After the overnight digestion at 37ºC and ligation, electroporation, using Bio-Rad Gene Pulser II system (400 Ω, 25 µF, 2.5 kV), into *E. coli* DH5-α was performed, originating vector pSG18-2.

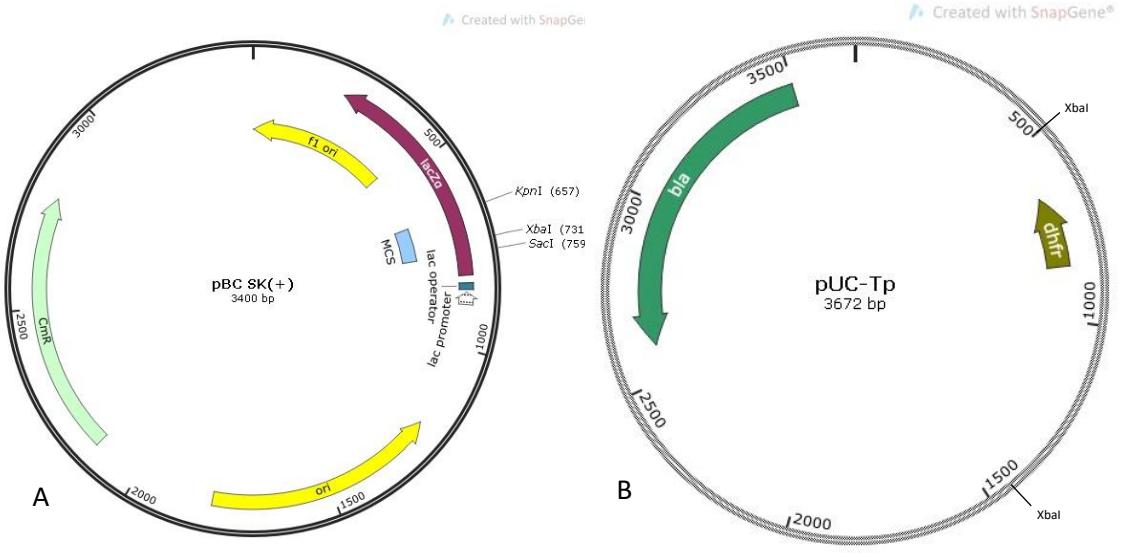

Figure 9. pBCSK⁺ and pUC-TP vectors used during the different cloning steps of *B. multivorans ΔldhA* constrution. pBCSK⁺ (A) is the basal vector in which the flanking regions were cloned into and, pUC-Tp (B) is the origin vector of the trimethoprim resistance cassette.

After cloning the first DNA fragment (upstream region containing *ldhR* gene) colonies containing the pSG18-1 vector were selected in solid LB medium with chloramphenicol 25 (25mg/ml), X-Gal and IPTG (LB+ Cm_{25} + X-GAL + IPTG). After cloning the second fragment the selection of the colonies containing the pSG18-2 vector was performed in LB + Cm25 growth media followed by Miniprep plasmid DNA extraction previously described.

To obtain the final vector (pSG18-3) containing the trimethoprim cassette flanked with the two previously amplified genes, both pSG18-2 and pUC-Tp vectors were digested with restriction enzyme *XbaI* followed by electroporation of *E. coli* DH5-α strain. *E. coli* cells were grown in LB medium supplemented with 100 mg/ml trimethoprim and 25 mg/ml chloramphenicol (LB $Tmp_{100}Cm_{25}$).

As a final step, triparental conjugation was performed. The receptor strain was *B. multivorans* P0213-1 isolate, the donor was *E. coli* DH5-α strain + pSG18-3 and the helper strain was helper plasmid pRK2013. Colonies capable of growing in LB medium supplemented with 250 mg/ml trimethoprim and 40 mg/ml gentamicin were selected.

Table 2. Vectors used during the several cloning steps of the mutant *B. multivorans ΔldhA* construction according to the flanking regions cloned into each one.

	Used Vector	Restriction Enzymes	Originated Vector
Upstream *(ldhR)*	$pBCSK^+$	KpnI/XbaI	pSG18-1
Downstream *(Bmul_2559)*	pSG18-1	XbaI/SacI	pSG18-2
Tmp Cassette	pSG18-2	XbaI	pSG18-3

2.4. Mutant confirmation

To confirm that the colonies obtained after the triparental conjugation step were in fact *B. multivorans* Δ*ldhA* mutant two different protocols were performed. The first strategy was based in PCR amplification of an internal region of 555 bp of *ldhA* gene. The used primers are the following:

Forward 5' – TTCAACCATGTCGACCTCGC – 3' and Reverse 5' – CTCTTCGTAGACGTCGAGGC – 3'. After PCR, amplification products were separated by agarose gel electrophoresis.

In a strategy it was assessed the ability of cells to decrease culture medium pH by secretion of lactate. For that, cells were inoculated in S medium supplemented with 2% D-Glucose. OD_{640nm} were taken, using HITACHI U-2000 spectrophotometer, for 72h alongside with the pH of growth medium. To this, 2 ml of suspension cells were removed from the growth culture being

1.9 ml centrifuged (Eppendorf centrifuge) so the pH of the supernatant was measured and the remaining 100 µl were diluted in 900 µl of water in order to take OD_{640nm}.

2.5. Complementation assays

Complementation assays were performed using triparental conjugation. The receptor strain was *B. multivorans* Δ*ldhA*, the donor was pARG015-1 (Silva et al., 2017) (a pBBR1MCS derivative containing a *HindIII* fragment expressing *LdhRA* from their own promoter) with the helper plasmid pRK2013. The selection occurred in LB medium supplemented with 200 mg/ml of chloramphenicol and 40 mg/ml of gentamicin.

2.6. Exopolysaccharide quantification

2.6.1. Liquid medium

The amount of exopolysaccharide produced was measured based on the dry weight of the ethanol-precipitated polysaccharide recovered from 50 mL cultures grown in EPS-producing medium (SM medium) for 2 days at 37°C with agitation at 250 rpm (Silva et.al 2017). The 50 mL cell suspensions were centrifuged for 15 minutes at 9000 rpm at 20°C and 150 mL of 96% ethanol was added to the supernatant to precipitate the polysaccharide. Results are the means of data from three replicates.

2.6.2. Solid medium

Mucoidy was assessed on yeast extract mannitol medium (YEM) containing 4 g/L mannitol, 0.5 g/L yeast extract and 15 g/L agar (Zlosnik et al. 2008). After inoculation, YEM plates were incubated for 48 h at 37°C and mucoid phenotype was then observed by visual inspection.

2.7. Biofilms formation

Bacteria were grown in LB medium at 37°C to mid-exponential phase and diluted to an OD_{640nm} of 0.05. 200 µL samples of the cell suspensions were used to inoculate 96-well polystyrene microtiter plates. Plates were incubated at 37°C statically for 48 h, after which the wells were washed three times with 0.9% (wt/vol) NaCl. The biofilm was stained with 200 µL of a 1% (wt/vol) crystal violet solution for 20 minutes at room temperature (Ferreira et al. 2007), followed by washing three times with 200 µL of 0.9% (wt/vol) NaCl. The dye was then solubilized with 200 µL of 96% ethanol and the solution's absorbance at 590 nm (A_{590nm}) was measured in a microplate reader (Spectrostar nano, BMG LabTech). Results are the means of data from at least twelve replicates of two independent experiments.

2.8. Growth under stress conditions and biomass estimation by dry weight

2.8.1. Minimal inhibitory concentration

Before subjecting the isolates to stressful conditions, it was necessary to understand which concentrations of each stress could lead to cell death. In the case of antibiotics, to identify the concentration needed to test if the antibiotic was capable of inducing cellular aggregates development, minimal inhibitory concentration (MICs) were estimated. The isolates were inoculated overnight in MH broth at 37ºC, 250 rpm. After this, optical density (OD_{640nm}) was measured using HITACHI U-2000 spectrophotometer and calculations were made, in order to inoculate an OD_{640nm} of 0.1 in 200 µl of MH broth in sterilized 96 wells plates. Several dilutions were performed, beginning at 256 µg/ml until 0 µg/ml, except in some strains in which higher concentrations needed to be tested in order to find the MIC, as explained at the results chapter. The 96 wells plates were inoculated overnight at 37ºC. Once again, after incubation the OD_{640nm} was measured with a dilution of 1:10.

2.8.2. Microscopic Observation

After the minimal inhibitory concentrations were determined, isolates were subjected to stressful growth media, SM medium supplemented with the several tested stresses and inoculated for 48h at 37ºC and 180 rpm.

To analyse the phenotypic changes after growth and, to understand which isolate was, or not, capable of producing cellular aggregates, microscopic observations were performed. Once cellular aggregates present large dimensions, low amplification (objective used 10x, from Zeiss Axioplan microscope). Photographs were taken in order to document all images that were visualized through Axiocam 503 color Zeiss camera adapted to the microscope. The program used to visualize the live images from the microscope and capture them was ZEN software.

2.8.3. Estimation of biomass in aggregates or as free cells by dry weight

After visualization of the phenotypic variations, quantification of the amount of aggregated and non-aggregated cells was performed. For this, a specific protocol was developed based on the protocol described by Haaber *et.al*. After incubation, in the previously described conditions, the growth cultures were transferred to 50 mL tubes and centrifuged at 1400 rpm at 20ºC for 30 seconds. After centrifugation, the suspensions rested for 10 minutes, without any movement, so the aggregates that were still in suspension could settle in the pellet. Then, the supernatant was removed by pipetting and placed in new 50 mL tubes, corresponding to the non-aggregated cells, that were centrifuged for at least ten minutes at 4000 rpm, so the non-aggregated cells could be separated from the growth medium. The resulting pellet was resuspended in the remaining five mL growth medium, and then several centrifugations, at 13200 rpm for two minutes, were performed in 2 mL eppendorf tubes in order to collect all cells from the same stress in the same tube. The suspensions containing the aggregates were also moved to 2 mL eppendorf tubes. After all the centrifugations, the 2 mL eppendorf are opened and stay at 60ºC until all the aggregates and non-aggregated cells are completely dried, presenting a brown colour. This process usually takes 72h, depending on the density of the presenting sample.

Before the samples are placed into Eppendorf tubes, these were weighted; the same procedure is performed after the samples are dried after the 72h at 60ºC.

2.9. Laboratory evolution experiment with isolate *B. multivorans* P0426-3

2.9.1. Growth conditions

Isolate P0426-3 was inoculated in SM medium for 30 days, at 37ºC and 180 rpm. Every two/three days 1 ml of the inoculum was re-inoculated in new SM medium as shown in Figure 10. After the 30 days 1 ml of the inoculum was serially diluted and plated onto solid LB medium. Different colonies were selected and inoculated in liquid LB medium and preserved in 30% glycerol at -80ºC.

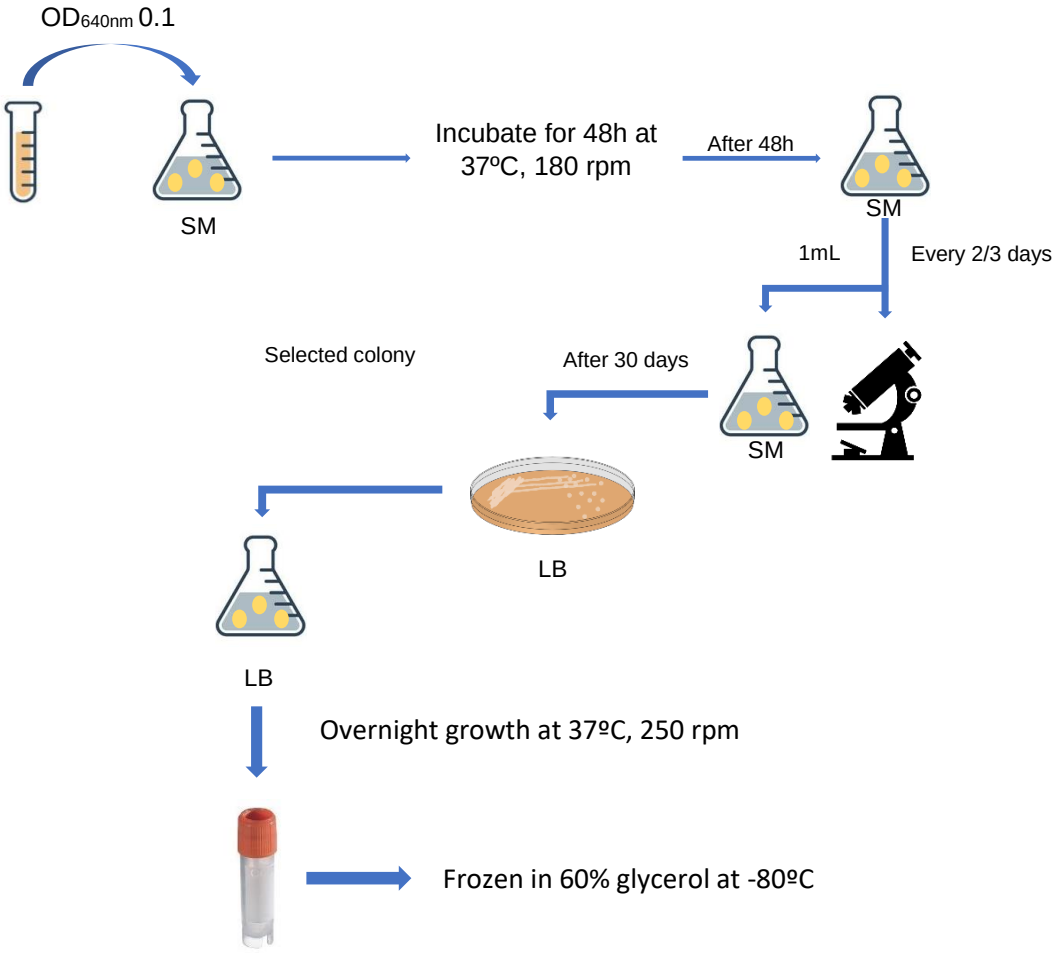

Figure 10 Representative scheme of the followed protocol during long-term laboratory evolution experiment.

2.9.2. Genome sequencing and detection of single-nucleotide polymorphism (SNP) mutations

Genomic DNA of *B. multivorans* P0426-3T30 mutant was extracted using the protocol previously described. The DNA sample was processed according to Illumina's instructions for generating paired-end libraries, which were sequenced using Illumina Nextseq system at Instituto Gulbenkian de Ciência (Portugal). To polish and filter reads, Sickle Filter reads software was used, followed by reference assembly. In this strategy the evolved P0426-3T30 reads were assembled against a previously sequenced P0426-3 isolate genome. To align the reads BWA v0.7.15 was used. After the alignment, gene prediction and annotation was performed with Prokka (Seemann 2014) program. A visual inspection of the alignments using Geneious v.6.1.8 (Kearse et al. 2012) allowed the confirmation of each indel and SNP mutations.

2.10. Statistical analysis

Statistical significance of differences in the data was determined using one-way analysis of variance (ANOVA) followed by Dunnett's multiple comparison test. The analyses were performed using GraphPad Prism v.5.04 software. Differences were only statistically significant for *P*-values lower than 0.05.

3. Results and Discussion

3.1. Intrinsic ability of *B. multivorans* clinical isolates to form cellular aggregates

The first aim of this study was to evaluate cellular aggregates formation by longitudinal series of *B. multivorans* recovered from cystic fibrosis patient's lung infections.

Together, we tested 129 isolates recovered from 9 CF patients, being 120 from the species *B. multivorans* and 9 from *B. pseudomultivorans*. The standard growth conditions included incubating cells in SM medium for 72h at 37ºC with 180 rpm of orbital agitation. Following this period, cultures were analysed macroscopically and microscopically for the presence and size of planktonic cellular aggregates.

3.1.1. Cellular aggregation in patient P0213 isolates

From patient P0213 were recovered 16 isolates in the period of 1996-2010. Macroscopic analysis of the 72 hours culture medium revealed the presence of many aggregates of sizes that can go up to 5 mm, in all isolates except P0213-13. This last isolate still produced aggregates, but very few in number and with a smaller size. Microscopic analysis of these aggregates showed highly branched structures resembling the root system of some plants (Figure 11). Despite some variation in this root-like structure among the different isolates, P0213-13 aggregates are more compact and not showing the branching pattern. From this analysis we conclude that the cellular aggregation trait was conserved during this chronic infection.

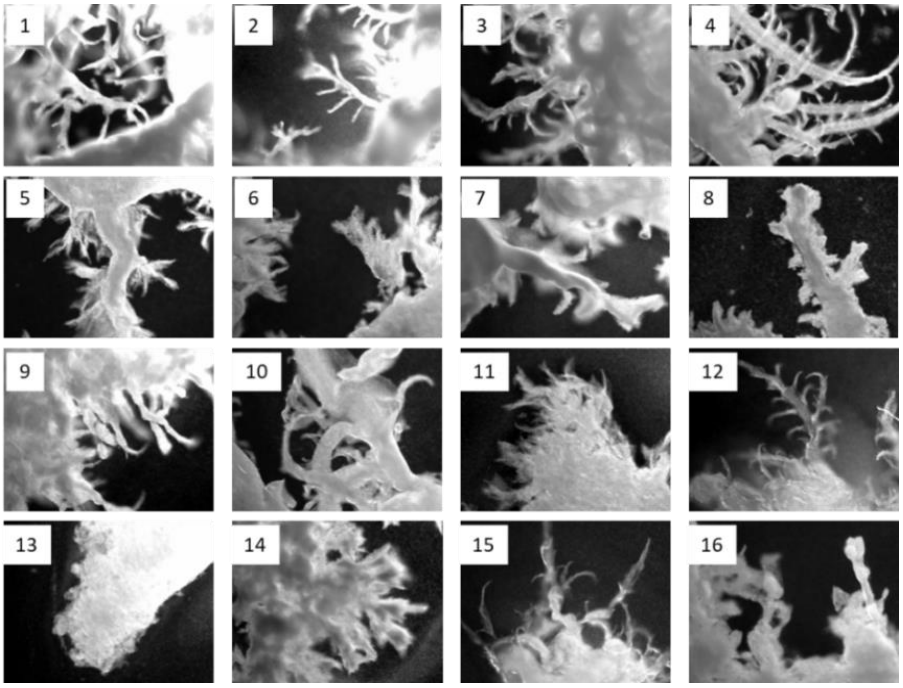

Figure 11 Microscopic images of the different 16 isolates recovered from patient P0213. Images have a magnification of 100x and were obtained with ZEN software. Each number in the image corresponds to each isolate number.

3.1.2. Cellular aggregation in patient P0342 isolates

During the period of 2004-2012 were recovered 10 isolates from patient P0342. Macroscopic analysis of the culture medium indicated that only isolates P0342-9 and P0342-10 were able to form visible aggregates. Nevertheless, when these cultures were visualized at the microscope, all except P0342-2 and P0342-3 were able to form aggregates (Figure 12). The estimated size of aggregates from P0342-1 and P0342-4 ranged from 37-46 µm, while from P0342-5, -6, -7 and -8 were smaller. These isolates have irregular shapes. In this patient, most of the isolates are able to form aggregates, and in the two last ones, this ability was even increased.

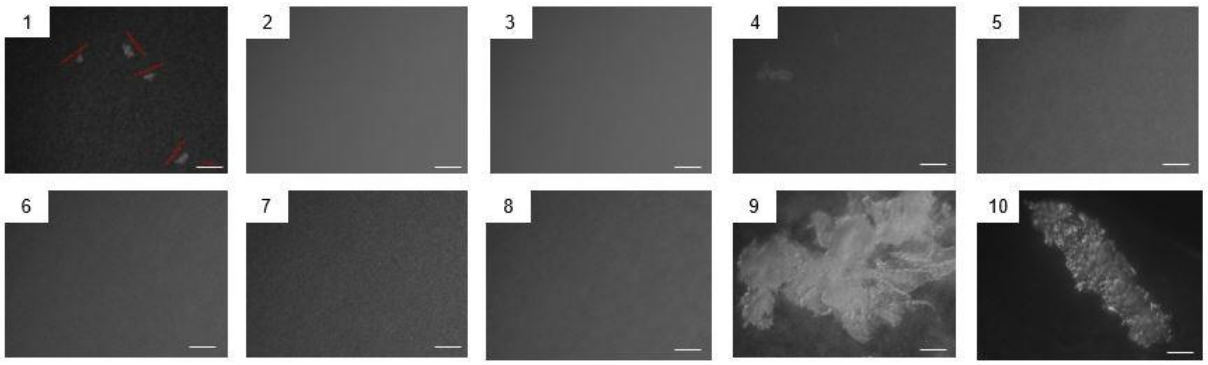

Figure 12 Microscopic images of the 10 different isolates recovered from patient P0342. Images have a magnification of 100x. All imagens were obtained using ZEN software. Each nunber corresponds to each isolate belonging to this patient. White bars correspond to the used scale during observations (100 µm).

3.1.3. Cellular aggregation in patient P0148 isolates

From patient P0148 it was recovered 11 isolates of *B. multivorans* in a seven years period (1989-1996). Analysis of the growth medium after 72 hours incubation allowed the visualization of macroscopic cellular aggregates in all isolates. Microscopic analysis revealed that isolates P0148-1, -2, -3, -6, and -8 produced aggregates of smaller size when compared with the remaining isolates (Figure 13). In general, these aggregates have irregular shapes with small ramifications. Isolate P0148-5 aggregates shows a slightly different structure with a more compact appearance and wider ramifications arising from the aggregate. Again, this trait was conserved in all isolates recovered from this long-term colonization of CF patient lungs.

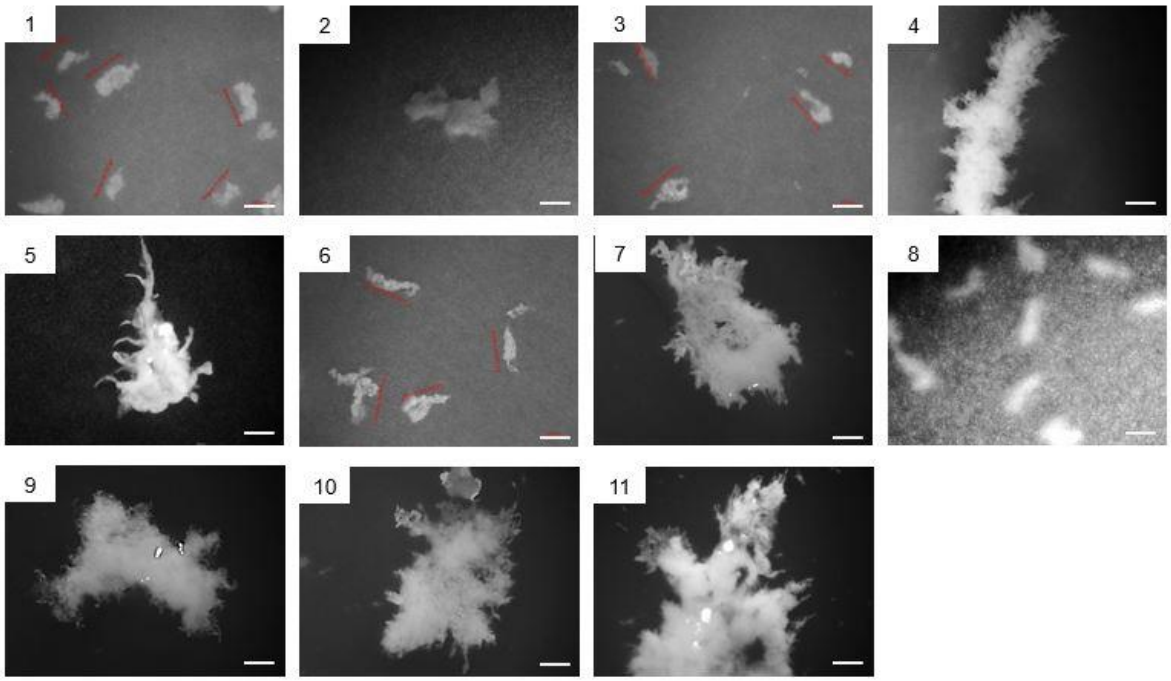

Figure 13 Microscopic images of cellular aggregates of the different 11 isolates recovered from patient P0148. Images of isolates 4, 5, 7, 9, 10 and 11 have a magnification of 40x. The remaining images have a magnification of 100x. Images were obtained using ZEN software. Each number represents the number of each isolate. White bars correspond to the used scale during observations (100 µm).

3.1.4. Cellular aggregation in patient P0205 isolates

From patient P0205 were recovered 23 isolates spanning a period of 22 years (1993-2015). Analysis of the growth medium after 72 hours did not reveal the presence of macroscopic aggregates. Nevertheless, when these cultures were visualized under the microscope, we found a group of strains where aggregates were indeed absent (P0205-7, -10, -13, -14, -16, -19, -20, -21, -22, -23) (Figure 14). The remaining isolates produce smaller aggregates with sizes up to 150 µm and irregular shapes. In this longitudinal series, cellular aggregates trait seems to be lost in the later isolates, at least under the tested conditions.

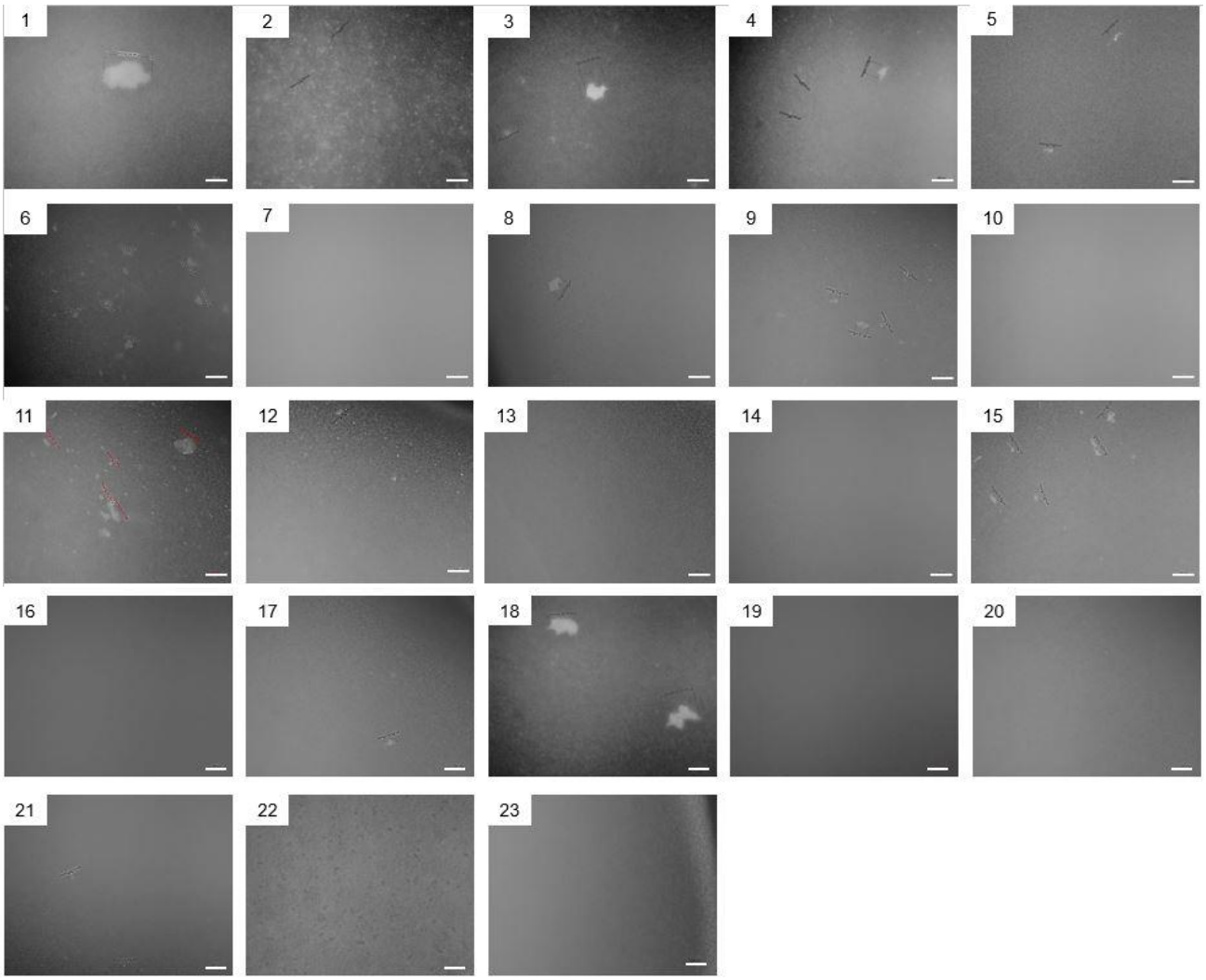

Figure 14 Microscopic analysis of the 23 different recovered from patient P0205. Images have a magnification of 100x and were obtained using ZEN software. Each number represents the number of each isolate. White bars correspond to the used scale during observations (100 µm).

3.1.5. Cellular aggregation in patient P0431 isolates

The 13 isolates from patient P0431 were recovered from the period between 1995-2008. Analysis of growth culture revealed the presence of macroscopic aggregates only in the first isolate, P0431-1. Nevertheless, microscopy images showed that isolates P0431-2, -3, -5, -7, and -9 also showed aggregates of small size (Figure 15). Cells from isolates P0431-10, -11, -12 and -13 seem to aggregate without producing stable structures.

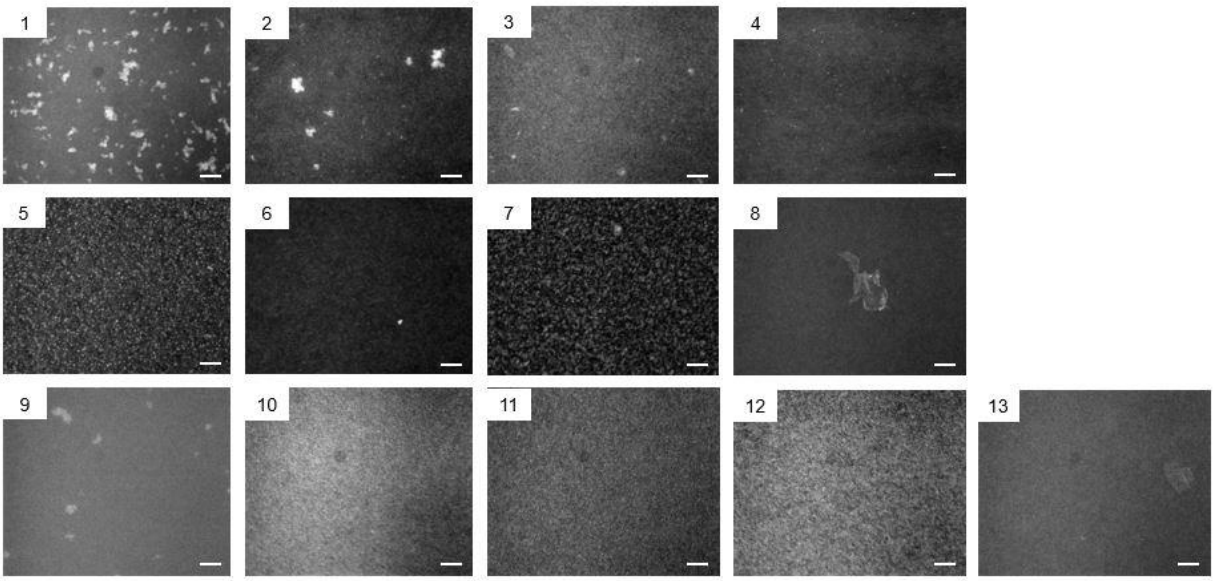

Figure 15 Microscopic observation of the 13 different isolates recovered from P0431 patient. Images have a magnification of 100x and were obtained with ZEN software. Each number represents the number of each isolate. White bars correspond to the used scale during observations (100 µm).

3.1.6. Cellular aggregation in patient P0280 isolates

Patient P0280 longitudinal series comprises 18 isolates recovered between 1995-2008. After 72 hours, growth medium showed that isolates P0280-1, -3, -6, -9, -11 and -12 are the only ones producing large cellular aggregates with sizes ranging 1 and 5 mm. Microscopic analysis confirmed the presence of these aggregates, but also revealed the presence of smaller aggregates (≈ 20 µm) in isolates P0280-2, -8, -10, -13, and -14 (Figure 16). Isolates P0280-4, -5, -7, -15, -16, -17, and -18 did not form aggregates under the tested conditions. Similarly, to the previous longitudinal series, this trait was conserved during chronic infection, but was absent in the later isolates.

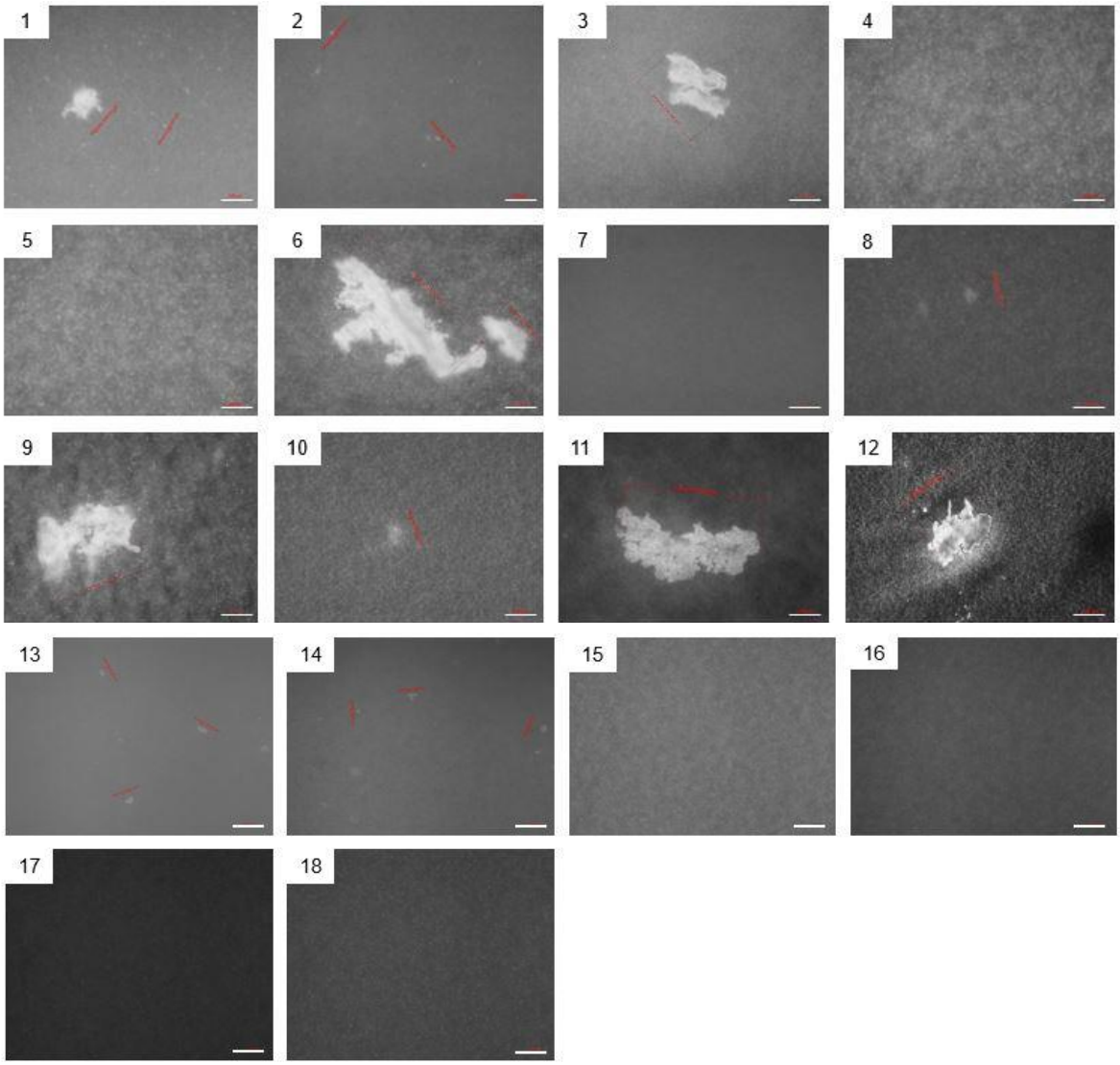

Figure 16 Microscopic observation of the 12 isolates recovered from patient P0280. Images have a magnification of 100x were obtained using ZEN software. Each number represents the number of each isolate. White bars correspond to the used scale during observations (100 µm).

3.1.7. Cellular aggregation in patient P0339 isolates

From the respiratory chronic infection of patient P0339 were recovered 6 isolates in an eight-year period (1995-2003). From these six isolates none produced macroscopic aggregates. Still, the microscopic analysis shown in Figure 17 confirms the absence of aggregates in isolates P0339-3, -5 and -6, but its presence in P0339-1, -2, and -4 (Figure 17). These isolates are of irregular structure, but the size of the first two isolates aggregates is larger than the ones produced by P0339-4 isolate.

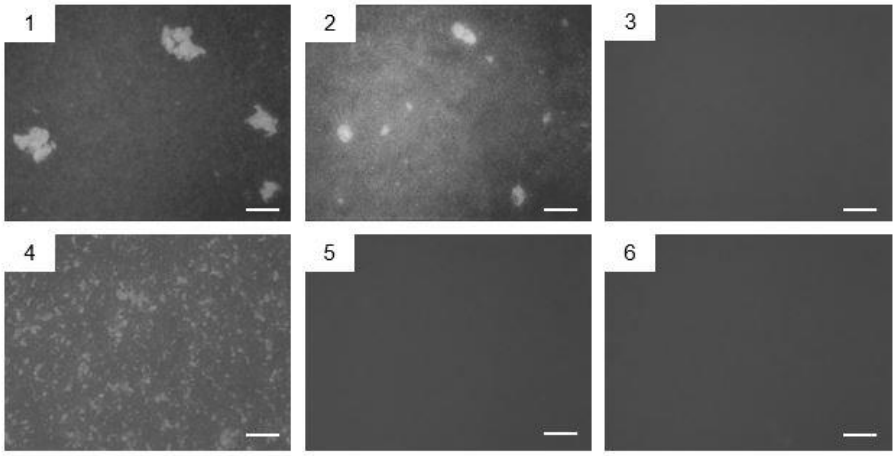

Figure 17 Microscopic imagens of cellular aggregates recovered from P0339 patient. Images have a magnification of 100x and were obtained using ZEN software. Each number represents the number of each isolate. White bars correspond to the used scale during observations (100 µm).

3.1.8. Cellular aggregation in patient P0426 isolates

The longitudinal series recovered between 1997 and 2014 from P0426 patient comprises 21 isolates. Macroscopic aggregates were only visualized in the cultures of P0426-1, -12, and -16. When the different growth cultures were analysed at the microscope two additional isolates had smaller aggregates, namely P0426-9 and P0426-17 (Figure 18). The remaining isolates did not allow aggregates visualization.

During the chronic lung infection of this patient, this trait was not conserved, being present in a minority of the isolates.

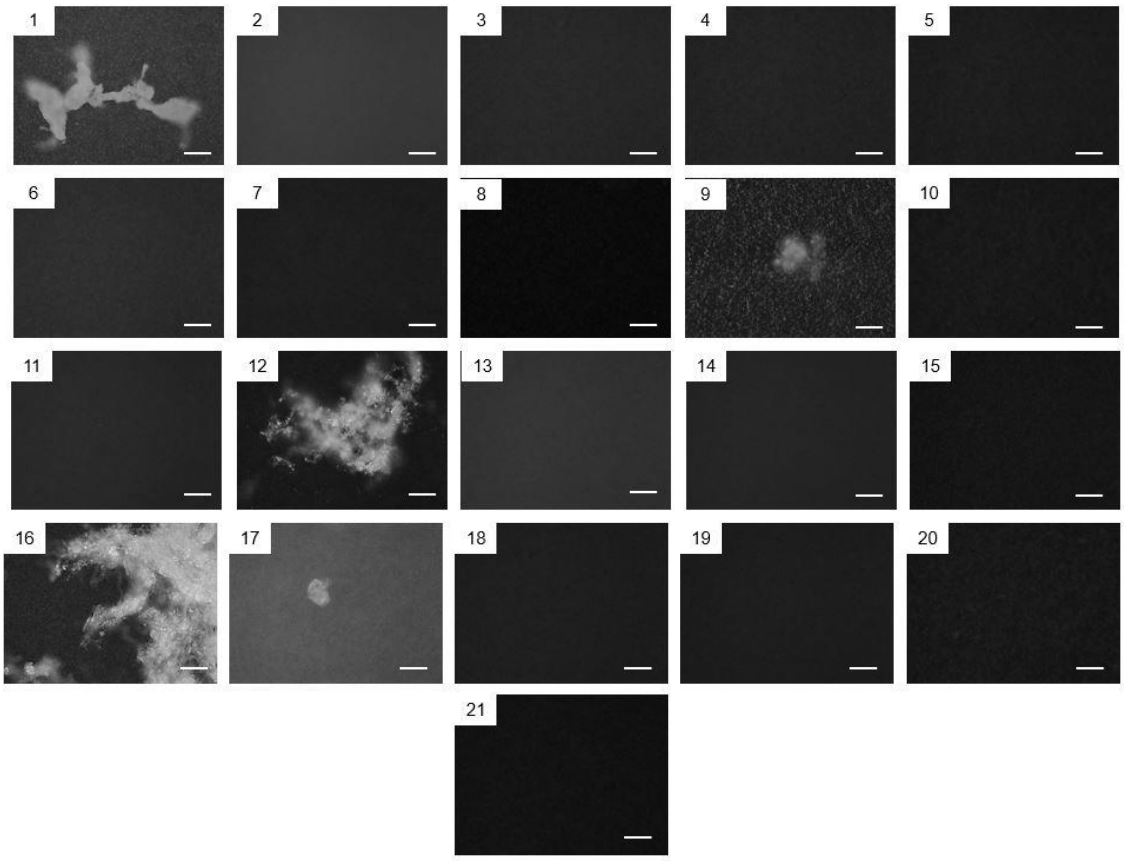

Figure 18 Microscopic images of cellular aggregates and non-aggregated cells of the 21 isolates recovered from P0426 patient. Images have a magnification of 100x and were obtained using ZEN software. Each number represents the number of each isolate. White bars correspond to the used scale during observations (100 µm).

3.1.9. Cellular aggregation in patient P0686 isolates

The longitudinal series of patient P0686 comprises 11 isolates. Isolates P0686-2 and P0686-3 are *B. multivorans* while the remaining isolates are *B. pseudomultivorans*. From all isolates only P0686-10 produced macroscopic aggregates. The microscopic analysis showed small aggregates in *B. multivorans* isolates, but except for P0686-10 isolate, none of the *B. pseudomultivorans* displayed this ability (Figure 19).

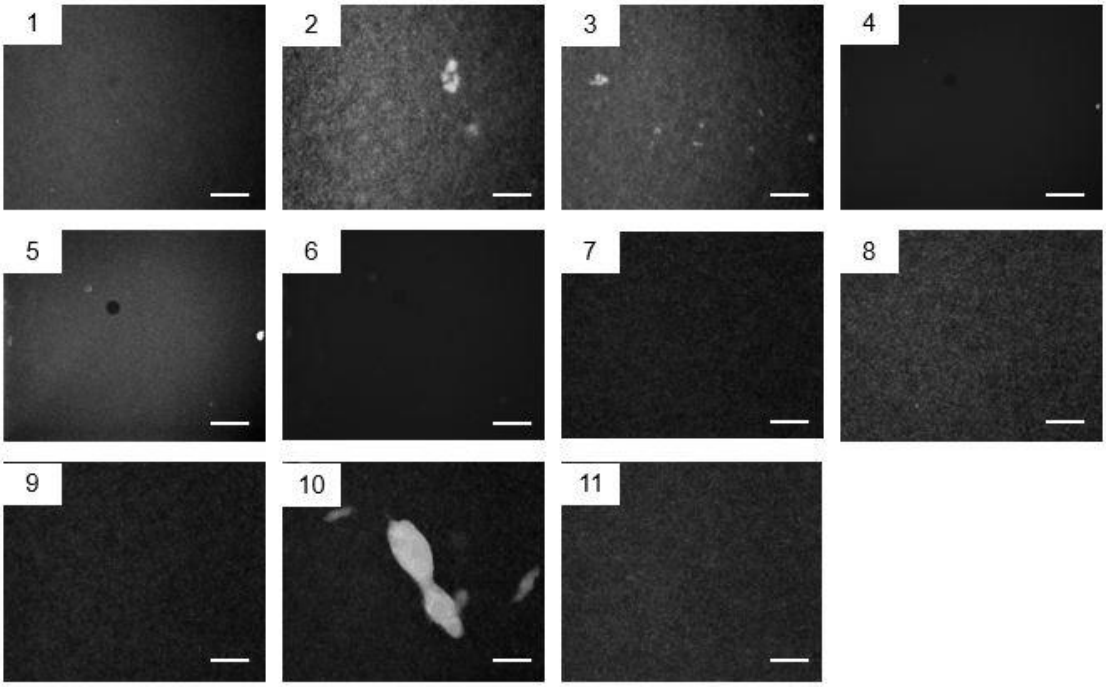

Figure 19 Microscopic images of cellular aggregates belonging to the 11 different isolates from patient P0686. Images have a magnification of 100x and were obtained using ZEN software. Each number represents the number of each isolate. White bars correspond to the used scale during observations (100 µm).

Results of this systematic analysis of aggregates formation ability in *Burkholderia multivorans* (and small set of *B. pseudomultivorans*) is resumed in Figure 20. This figure shows that the majority of the isolates form cellular aggregates when grown in a medium with high C/N ratio; this trait is conserved during long periods of respiratory infection and, when lost, it happened more frequently in late isolates.

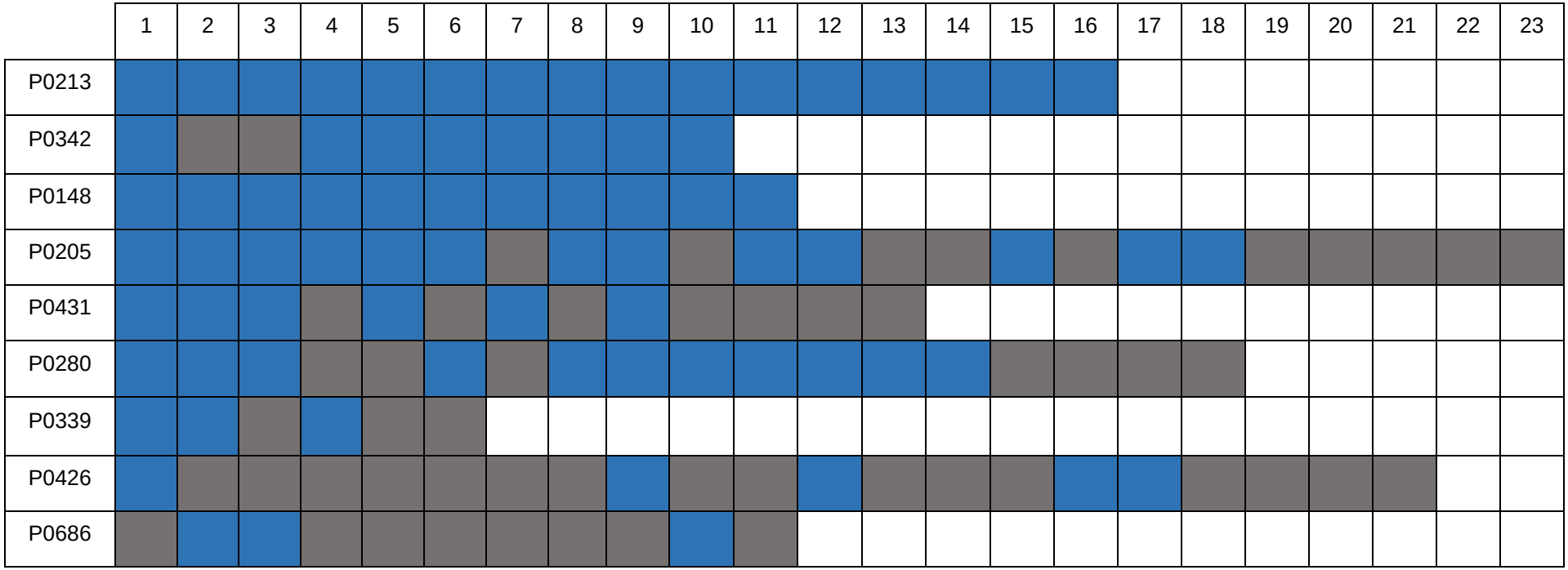

Figure 20 Schematic representation of isolates ability to produce cellular aggregates in SM medium. Blue squares represent the ability to produce cellular aggregates, whereas grey squares represent the inability to produce such structures.

3.2. Environmental conditions triggering aggregates formation

After having demonstrated the ability of clinical isolates of *B. multivorans* to form cellular aggregates in SM medium, it is our aim to investigate whether this trait changes with different media or under different stress conditions. To do that, there is the need to develop an experimental procedure for quantification of cellular aggregates. One possibility was to use a sieve that retains aggregates, but it turned out to be impossible to remove aggregates from the sieve. Also, it would not retain smaller aggregates. Therefore, it was tested a different method which includes centrifugation at low centrifugation force to pellet aggregates, removal of the free cells to a new tube, followed by centrifugation at high centrifugation force; dry both cellular pellets at 60ºC; and weight them. The percentage of aggregates refers to the total weight of cells.

3.2.1. Influence of growth medium in cellular aggregates formation

Due to the high number of clinical isolates that we have analysed, it would be impractical to continue with all of them. Therefore, the following experiment only include isolates P0213-1, P0342-1, P0342-2, P0342-3, P0148-1, P0148-3, P0148-6, P0205-1, P0205-7, and P0205-10. From this list, P0342-2, P0342-3, P0205-7 and P0205-10 were unable to form cellular aggregates in SM medium as previously shown by the microscopic analysis.

Quantification of aggregates from the referred isolates grown in SM medium at 37ºC, 180 rpm for 48 hours shows that in P0213-1 isolate, 61.6% of the cells are present as aggregates (Figure 21), confirming the high ability to form this type of structures. In the other isolates, which do form aggregates in SM medium (P0342-1, P0148-1, P0148-3, P0148-6 and P0205-1), this value is below 8%. The remaining isolates (P0342-2, P0342-3, P0205-7 and P0205-10) show values below 1%, which we will consider a value of no aggregation. Since this quantification method nicely reproduced the macroscopic and microscopic evaluation previously done, we consider it appropriate for the remaining studies.

SM medium is a salts medium with high ratio of C/N and, might be stressful for cells when nitrogen sources became limited. Therefore, we tested whether a more equilibrated and richer medium such as LB would have a negative impact in cellular aggregation. Data shown in Figure 21 confirmed the reduction of cells in the form of aggregates for P0213-1, all P0148 isolates, and P0205-1, but not for P0342-1 isolate. Isolates P0205-7 and P0205-10, which were unable to aggregate in SM medium, are also unable to aggregate in LB medium. Against this trend are the isolates P0342-2 and P0342-3 which are producing aggregates in LB but not in SM. Images of the aggregates formed by P0342 isolates are shown in Figure 21 B. Overall, we can conclude that growth in LB medium leads to lower aggregation of cells, but there are exceptions.

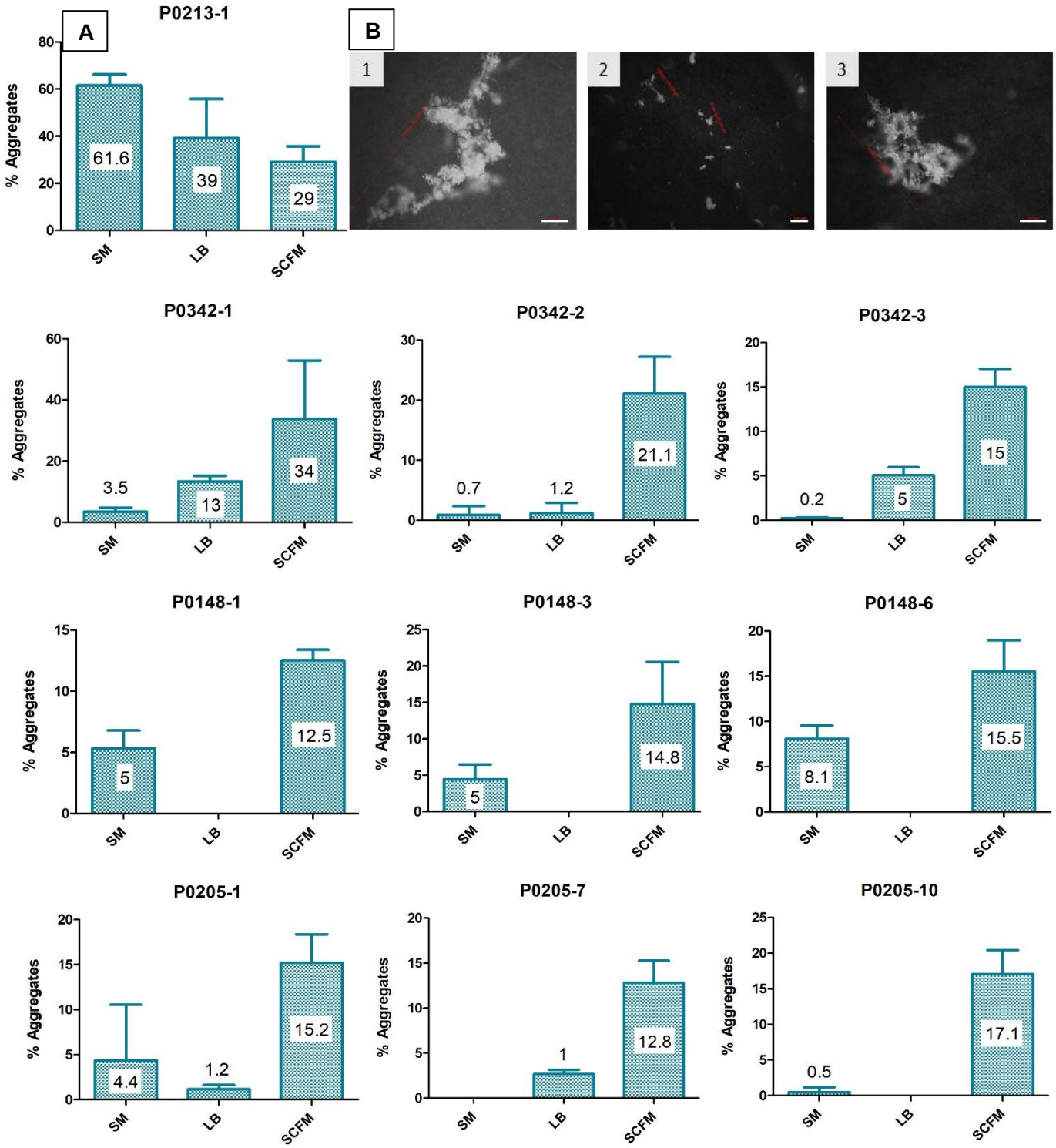

Figure 21 A – Percentage of cells in the form of aggregates as estimated by dry weight in the chosen isolates from the 9 patients after growing in different growth medium. Error bars correspond to the standard deviation of the means of at least 3 different replicas; **B** - Cellular aggregates of patient P0342 isolates after growth in LB medium. Images have a magnification of 100x and were obtained with ZEN software. White bars correspond to the used scale for cellular aggregates measurement (100 µm).

Because SM and LB media do not mimic the lung environment, we decided to use synthetic cystic fibrosis medium (SCFM) developed by Palmer et al (2007). Besides salts, this medium contains

all amino acids and, is thought to be closer to the CF lung environment. Isolates under study were grown for 48 hours at 37ºC, 180 rpm. Results from Figure 21 indicate that all of them are able to form aggregates in this medium, and except for P0213-1, the percentage of aggregates increased considerably.

Microscopic analysis of the 48 hours growth cultures is shown in Figure 22. P0213-1 still forms macroscopic aggregates with many ramifications, but with a structure less compact than in SM medium (Figure 22 A). Microscopic analysis of the culture (excluding large aggregates) shows many smaller aggregates that can measure up to 400 µm (Figure 22 A1).

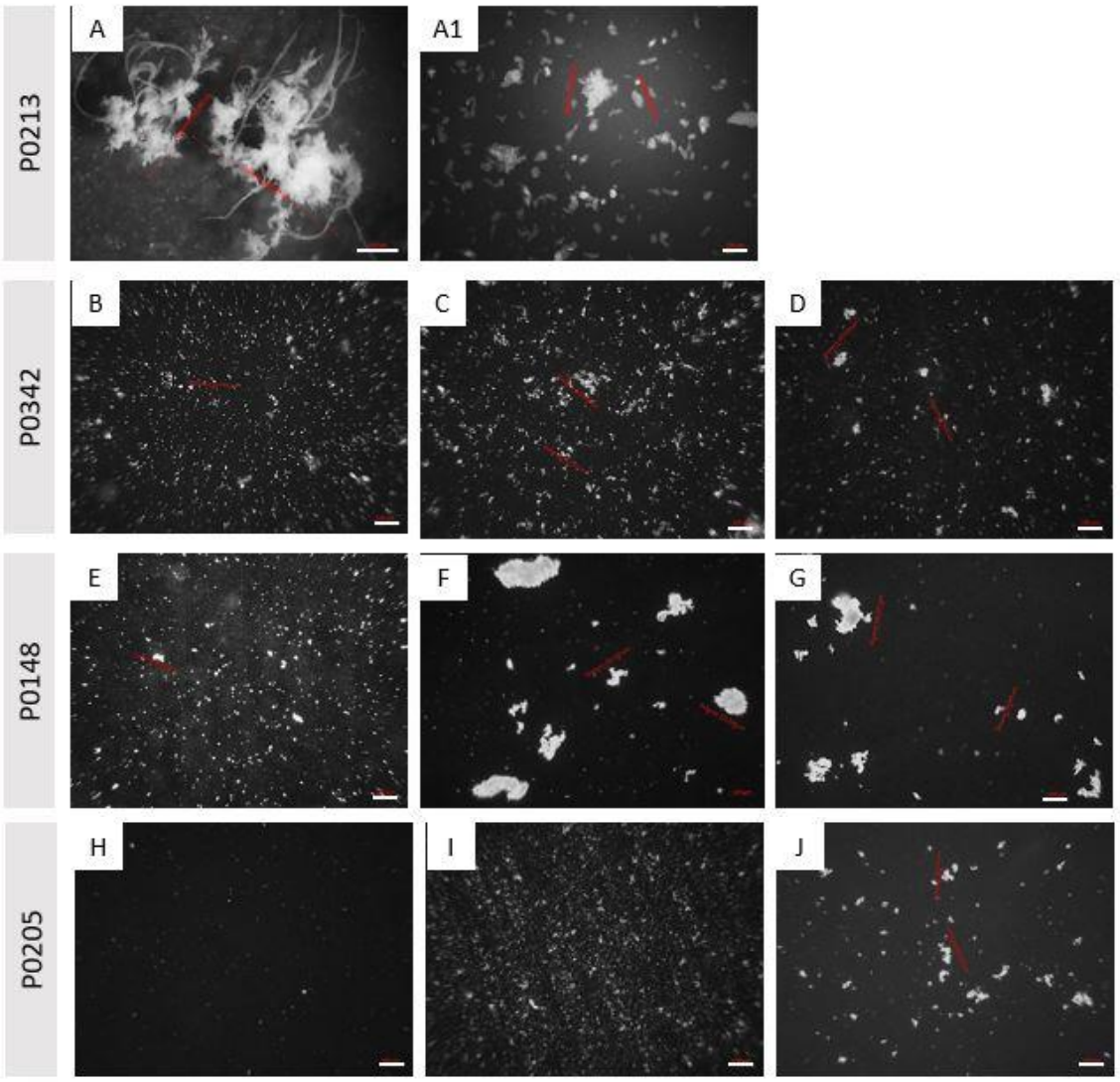

Figure 22 Microscopic images of cellular aggregates produced the different patients when grown in SCFM medium. Image A has a magnification of 25x and, images A1- J have a magnification of 100x and, were obtained using ZEN software. White bars correspond to the used scale during observations (500 µm and 100 µm, respectively).

P0342 isolates have aggregate sizes between a few micrometres up to 100 µm (Figure 22, B-D). P0148 isolates have differences in the sizes of the aggregates, with P0148-1 aggregates being smaller (below 50 µm) than the two other isolates which can go to 450 µm in P0148-3 and 160 µm in P0148-6 (Figure 22 , E-G). From the last group of isolates analysed, P0205-7 and P0205-10 produce

aggregates no bigger than 100 µm, while in P0205-1, these aggregates are even smaller (Figure 22, H-J).

With this set of experiments here described, we can conclude that the composition of the growth medium is determinant for the outcome of cellular aggregation. LB medium, being perhaps more balanced, leads to a lower number of strains being able to aggregate. SM medium induced the formation of aggregates possibly due to nitrogen limitation. In *Azospirillum brasilense* it has been reported that nitrogen limitation triggers cellular aggregation (Bible et al. 2015), suggesting that this might be the reason for increased *B. multivorans* aggregation. The last tested medium, SCFM, was the one with stronger impact in the number of isolates being able to form aggregates. A previous study where *Pseudomonas aeruginosa* was grown in artificial sputum medium rich in amino acids showed the ability of these microorganisms to form microcolonies (Sriramulu et al. 2005). Contrastingly, in a medium without amino acids, no microcolonies were observed, leading to the hypothesis that amino acids might be the cause for this difference. It would perhaps be interesting to deplete the SCFM with one amino acid at a time to see whether some amino acid(s) is relevant.

3.2.2. Stress conditions triggering cellular aggregates formation

The aim of this section is to evaluate if different stresses affect cellular aggregates formation. The chosen stresses are: sub-inhibitory concentration of ciprofloxacin, excess of nitrogen source, Mg^{2+} limitation, oxidative stress caused by H_2O_2 and osmotic stress.

Ciprofloxacin is a second-generation quinolone inhibiting DNA topoisomerases and DNA gyrase and, is frequently administered to CF patients with respiratory infections. Therefore, it was considered an interesting antimicrobial for the purpose of this work. But before incubating cells in its presence we had to determine the minimal inhibitory concentration (MIC) for each of the selected isolates. As described in the material and methods section, the MIC values were determined. But, since the aim was to stress cells and not kill them, the concentration of ciprofloxacin used was bellow this value. Table 3 shows the concentration of antibiotic used.

Table 3 Minimal Inhibitory Concentration (MIC) values and antibiotic concentrations used during the study to stress the different isolates.

Antibiotic / Isolate	MIC value (µg/mL)	Ciprofloxacin (µg/mL)
P0213-1	1	1
P0342-1	0.25	0.125
P0342-2	0.25	0.125
P0342-3	0.25	0.125
P0148-1	0.125	0.125
P0148-3	0.25	0.125
P0148-6	0.5	0.125
P0205-1	0.5	0.25
P0205-7	0.5	0.25
P0205-10	0.5	0.25

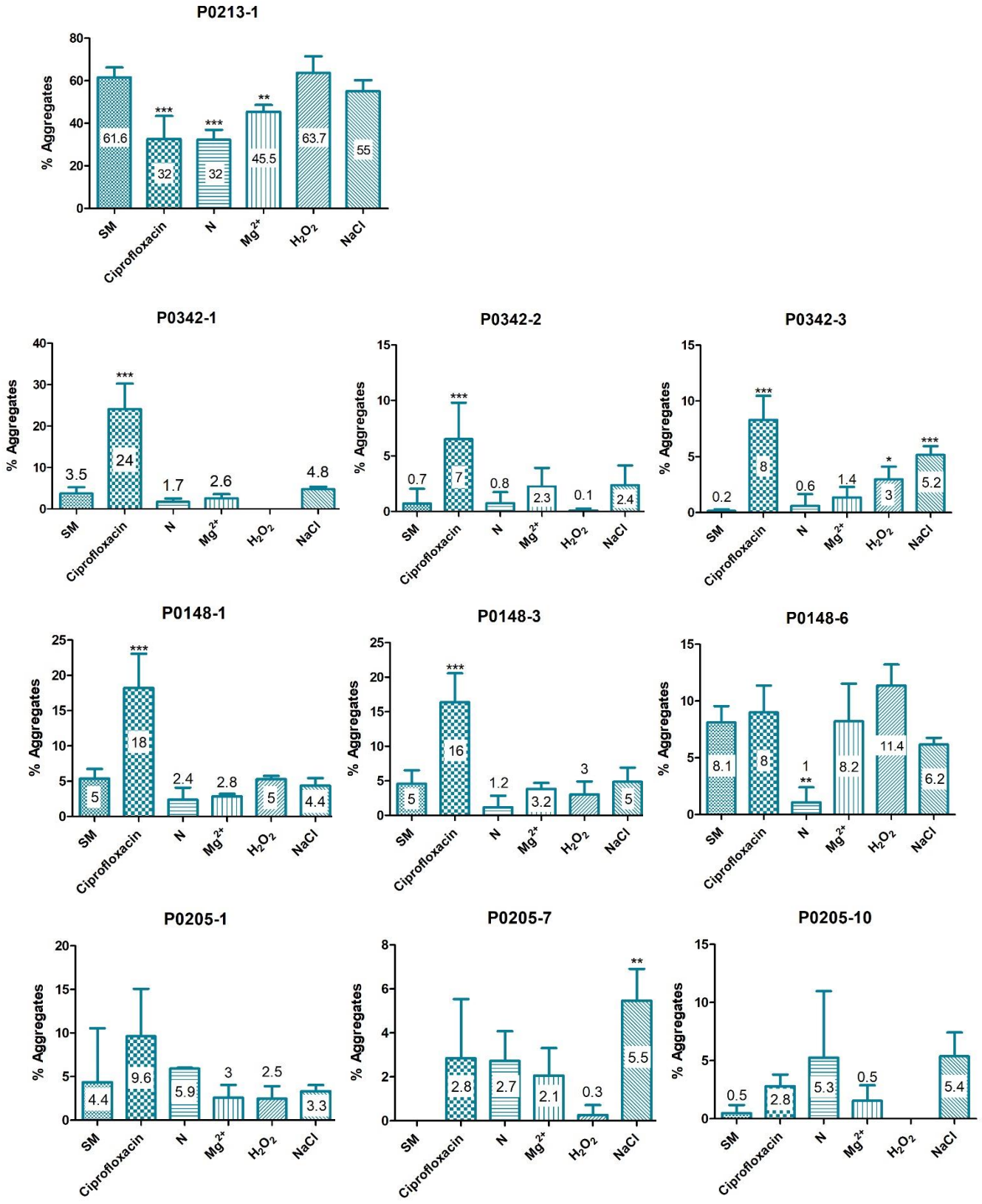

Figure 23 Percentage of cells in the form of aggregates as estimated by dry weight in the chosen isolates belonging to the 9 different patients after a 48h growth under the several stress conditions. Error bars correspond to standard deviation of the means of at least three different replicas. Statistical analysis between stress and control conditions was performed using one-way ANOVA Dunnett's test. Only results with statistical significance *P*-value<0.05 were considered significant. (*, *P*-value<0.05; **, *P*-value<0.01; ***, *P*-value<0.001).

Each culture was then incubated in SM medium supplemented with the sub-inhibitory concentration of ciprofloxacin at 37ºC for 48 hours and 180 rpm. The percentage of cells found as aggregates was determined and results are shown in Figure 23. When compared with SM medium only, all isolates except P0213-1 showed increased percentage of biomass in the form of aggregates. This is also true for isolates P0342-2, P0342-3, P0205-7 and P0205-10 which did not form aggregates in SM but can do it in the presence of ciprofloxacin. Microscopic images showing aggregates formed by P0342 isolates is shown in Figure 24.

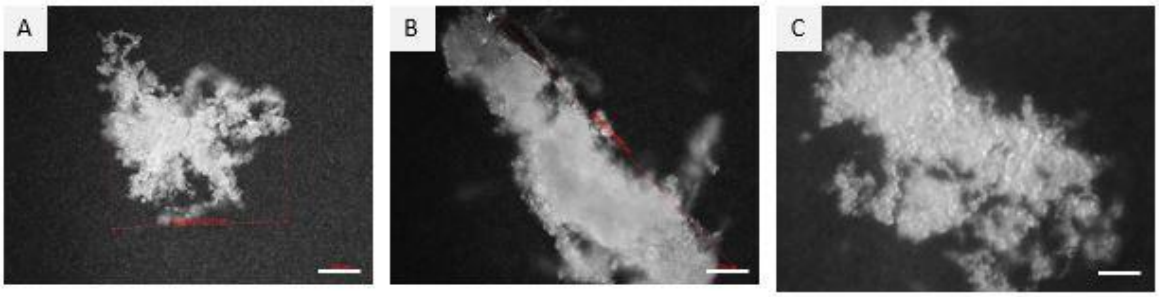

Figure 24 Microscopic images of cellular aggregates belonging to the three selected isolates from patient P0342 after a 48h growth in SM medium supplemented with ciprofloxacin. Images have a magnification of 100x and were obtained using ZEN software. (A) - P0342-1, (B) - P0342-2; (C) - P0342-3. White bars correspond to the used scale for cellular aggregates measurement (100 µm).

The presence of ciprofloxacin leads to an increase of DNA scission rates and inhibition of the ability of topoisomerase to re-ligate cleaved DNA (Anderson et al 1998), which will decrease cell replication and transcription (Hangas et al. 2018). To combat the negative effects of the antibiotic, cells in the proximity will aggregate. Inside these aggregates, concentration gradients are established (Zhang et al. 2011), promoting resistance against stressful environments. It is possible that by creating a gradient in the aggregate, cells would be protected from the negative effects of the antibiotic.

Since in *Azospirillum brasilense* high concentration of nitrogen was also stressful for cells (Bible et al. 2015), we tested whether increasing casaminoacids from 1g/L to 5g/L would benefit cellular aggregation. The results obtained differed significantly between isolates. While for P0213-1 and all P0148 isolates we observed a negative effect on aggregation, in P0342 isolates there was no difference between the two conditions (Figure 23). The positive effect on aggregation was only visible for P0205 isolates, but the huge error bars prevent solid conclusions. The most likely explanation is that the amount of casaminoacids was not stressful al all, most likely the opposite. If this has to be included on the list of possible stressors affecting cellular aggregates formation, then higher concentration has to be used.

Magnesium is an important activator of cellular enzymes involved in several metabolic pathways, such as the glycolytic and glyoxylate pathways (Cowan 2002). To study the effect of magnesium limitation in cellular aggregates formation, the Mg^{2+} concentration in SM medium was reduced from 8 to 0.02 mM. Data from Figure 23 shows a general negative effect on aggregation. Microscopic images

confirm that isolates that do not form aggregates in SM also do not form in SM medium depleted from Mg^{2+}. Overall, under the tested conditions, magnesium limitation did not trigger cellular aggregation, but perhaps we are not under limiting conditions since other components of SM medium might have traces of this ion.

Another stress under study was oxidative stress generated by hydrogen peroxide. Since *Burkholderia* is known to be highly sensitive to this compound, a very low concentration (0.005 % (v/v)) was used. As shown in Figure 23, there are no significant differences between SM and SM supplemented with H_2O_2, perhaps with the exception of P0342-3 which did not produce detectable aggregates in SM, but does it in the presence of H_2O_2. In this experiment, it was observed some growth arrest in the first hours and only then growth resumed. Perhaps lower concentrations of H_2O_2 should be tested.

The last stress condition imposed to the isolates under study was osmotic stress. For that, instead of normal 1g/L of NaCl in SM medium, we added 10 g/L. The effect in cellular aggregation was strain specific. No significant differences were observed for P0213-1 and for P0148 isolates, while P0342 and P0205 isolates increased the amount of biomass in the form of aggregates (Figure 23).

In a previous study on the response to osmotic stress by *Burkholderia*, Behrends et al (2011) concluded that each strain responds differently. In their study, they demonstrated that several metabolites such as alanine, phenylalanine, glutamate, trehalose and glycine-betaine can be produced and grouped as osmotic tolerance strategies into three categories: I – isolates that induce metabolic changes in response to osmotic stress by increasing the levels of all osmo- responsive compounds; II – isolates where only amino acids increase their levels, but the production of glycine-betaine and trehalose is null; and III – isolates where only glycine-betaine levels increase. It is then possible to conclude that each strain may respond differently to this stress and that also impacts differently their aggregation phenotype.

Taken together, our results show that sub-inhibitory concentration of ciprofloxacin is the best trigger of cellular aggregates formation. Other stresses such as oxidative and osmotic stresses might also have an impact, but it seems to be more strain-specific.

4. Deletion of *ldhA* gene from *B. multivorans* P0213-1 genome and its impact on aggregates formation

4.1. Construction of *ldhA* mutant

In *B. multivorans* ATCC 17616, gene *ldhA* encoding lactate dehydrogenase is co-transcribed with *ldhR* encoding a LysR-type transcriptional regulator (Silva et al 2017). As referred in the introduction, both genes have been demonstrated as strongly implicated in planktonic cellular aggregates formation. Since identical genetic organization was found in *B. multivorans* P0213-1 (Figure 25 A) it was decided to create a deletion mutant to assess the importance of this gene in the phenotype under study.

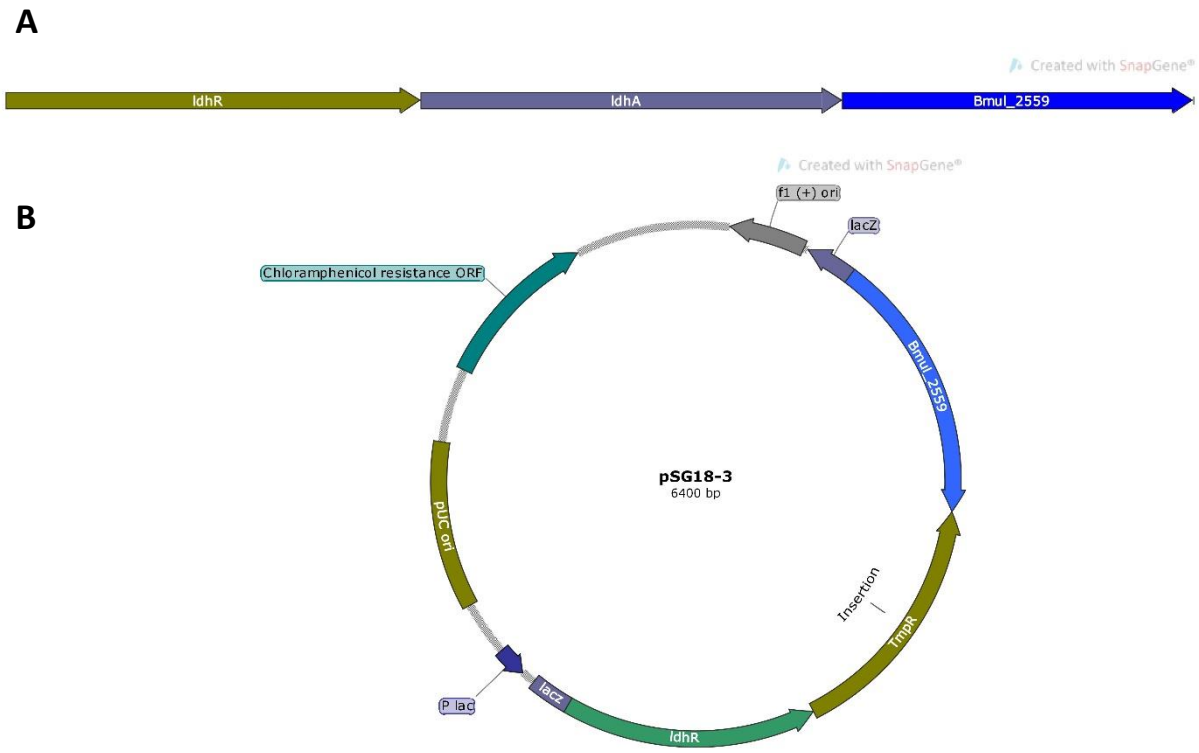

Figure 25 A – Genetic organization of *B. multivorans* P0213-1 region containing *ldhA* gene and flaking region; **B** - Constructed vector with the genes up and downstream the *ldhA* gene, and the trimethoprim cassette cloned into de vector pBCSK+. Images were design using SnapGene software (from GSL Biotech; available at snapgene.com).

The general strategy was to clone the flanking regions of *ldhA* gene into pBCSK$^+$ and clone a trimethoprim resistance cassette in the place occupied by the *ldhA* gene. This construction is shown in Figure 25 B and was named pSG18-3. This plasmid was mobilized into P0213-1 cells and recombinants were selected in LB supplemented with trimethoprim 250 mg/L and gentamicin 40 mg/L. The obtained colonies were then counter selected in the presence of chloramphenicol to find the double recombinants (the ones that were chloramphenicol sensitive). One colony was obtained and tested by PCR for *ldhA* gene amplification. If *ldhA* gene was present we should obtain a 555 bp fragment, what was effectively confirmed for the wild-type strain as shown in Figure 26. From the

mutant, several bands can be seen, but none has the expected size. This mutant was named P0213-1 Δ*ldhA*.

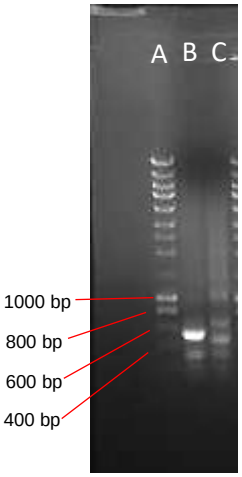

Figure 26 Electrophoresis in agarose gel from amplified *ldhA* 555 bp region. At left is the standard NZYDNA Ladder III (A), in the middle is P0213-1 (B) and in the right is Δ*ldhA* (C). The image was obtained using imaging software Quantity One 4.5.2 from BIO RAD (BIO RAD Universal Hood II). To visualize any amplicons, it was used a transilluminator with UV light and the 0.8% agarose gel was previously stained with GreenSafe® (Nzytech, Portugal).

4.2. Growth of P0213-1 Δ*ldhA* mutant in S medium supplemented with glucose

A hallmark of *ldhA* mutation in *B. multivorans* ATCC 17616 is the fact that this mutant, when growing in the presence of 20 g/L glucose, does not acidify the medium as much as the wild-type strain (Silva et al 2017). As a consequence of no lactate secretion cells remain viable while wild-type cells lose their viability. To assess if this phenotype is maintained in P0213-1 and P0213-1 Δ*ldhA* mutant, both were grown in S medium with 2% D-glucose and the optical density and culture medium pH measured for 72 hours.

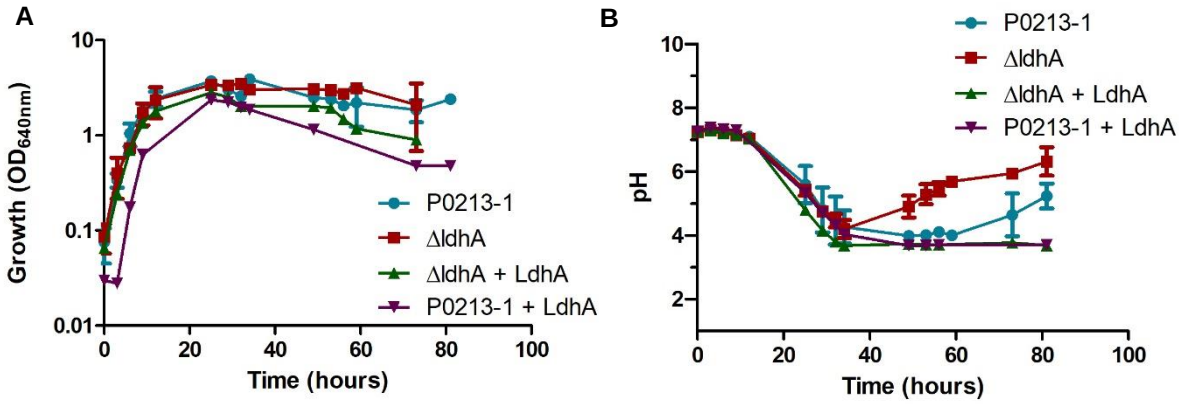

Figure 27 Culture growth measured by turbidity (OD_{640nm}) of the WT strain (*B. multivorans* P0213-1), mutant strain (*B. multivorans* Δ*ldhA*), wild-type expressing extra copies of *ldhA,* and complemented mutant, in 2% D-Glucose (A). Culture medium pH in 2% D-glucose S medium is shown (B).

Regarding the optical density, there are no major differences between wild-type and mutant, although the mutant reached slightly higher values in stationary phase (Figure 27 A). Analysis of the extracellular pH indicates that until 34 hours of growth both wild-type and Δ*ldhA* mutant decrease the pH value to 4.6 and 4.4, respectively (Figure 27 B). After this time point the culture medium pH of the mutant increased to neutrality while the one of the wild-type remained constant up to 60 hours and then started to increase. The behaviour of this wild-type strain differs from the *B. multivorans* ATCC 17616 since in this last one there was a stronger pH decrease to 3.9 and no recovery (Silva et al 2017). Despite that, this result suggests that *ldhA* mutant of P0213-1 most likely does not produce lactate.

To demonstrate that the phenotype of the mutant was caused by ldhA mutation, we overexpressed *ldhA* and *ldhR* from plasmid pARGO15-1 (Silva et al 2017) in the wild-type and mutant strains. As shown in Figure 27 A, both strains showed decreased optical density in stationary phase and, the culture medium reached lower pH and, consequently, it did not recover to higher values since cells lost viability (Figure 27 B). In conclusion, the level of lactate dehydrogenase activity in the wild-type strain grown in the presence of glucose does not have a negative impact in cells growth, but if additional copies of this gene are introduced, lactate production increases, pH decreases, and cells viability decreases.

4.3. Role of LdhA in cellular aggregates formation

To evaluate whether D-lactate dehydrogenase LdhA from P0213-1 also plays a role in cellular aggregation, wild-type and mutant were incubated in SM medium and grown for 48 hours at 37ºC, 180 rpm. Macroscopic analysis of the two cultures showed lower number of aggregates in the Δ*ldhA* mutant, which also presented smaller size. Microscopic analysis of the aggregates showed the same

type of root-like structure already described (Figure 28). Size estimation of the several isolates indicated values over 1000 µm for the wild-type while the mutant aggregates had less than 600 µm. Quantification of aggregates and free cells confirm a reduction of biomass present in the form of aggregates by the Δ*ldhA* mutant (Figure 29). Overexpression of LdhA in the mutant strongly increased the amount of aggregates, with the value reaching approximately 97% while the mutant showed 46% and the wild-type 62%, as determined from the dry weight of biomass.

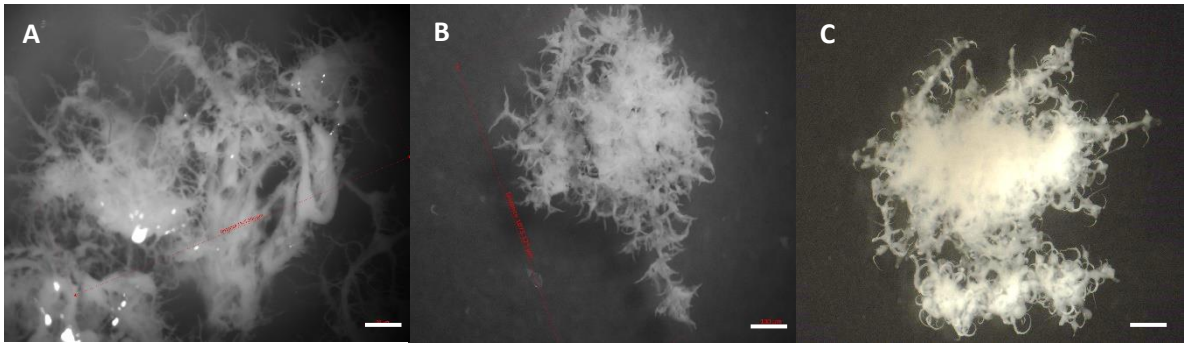

Figure 28 Cellular aggregates produced by P0213-1 (A - wild-type), *ΔldhA* (B - mutant) and complemented mutant (C - complemented) when grown in S medium with 2% D-mannitol for 48h at 37ºC and 180 rpm. The three images were obtained by magnifier observation using ZEN software. (A) – Image have a magnification of 32x, and the presented aggregate has a size of 1105.355 µm; (B) – Image have a magnification of 25x, and the cellular aggregate presented has a size of 1073.125 µm; (C) – Image have a magnification of 20x. White bars correspond to the used scale for cellular aggregates measurement (100 µm).

As previously said, in *P. aeruginosa* the two-component regulator MifR is responsible for micocolonies formation (Petrova et al. 2012). However, such phenotype is also dependent of pyruvate fermentation, once the inactivation of genes encoding lactate dehydrogenase led to phenotypes similar to those observed in *mifR* mutants (lack of cellular aggregates). It is thought that within cellular aggregates cells experience oxygen-limiting and energy-rich conditions leading to pyruvate fermentation as a way of maintaining redox balancing, (Silva et al 2017; Petrova et al. 2012). According to Silva et. al (2017) the contribution of *B. multivorans* ATCC 17616 D-lactate dehydrogenase in cellular aggregates formation may be also due to the anoxic environment within the aggregates, inducing cells to ferment pyruvate (the process involves the conversion of pyruvate into lactate) as a way of redox balancing. With this, it would be expected the production of smaller cellular aggregates by Δ*ldhA* mutant when comparing with the WT strain. This is in line with the present results, since the decrease of cellular aggregates production can be a consequence of the absence of pyruvate fermentation. It was also possible to conclude that LdhA activity contributes to cellular aggregates formation, however it is not the only factor contributing to this phenotype, as the mutant strain continues to produce cellular aggregates.

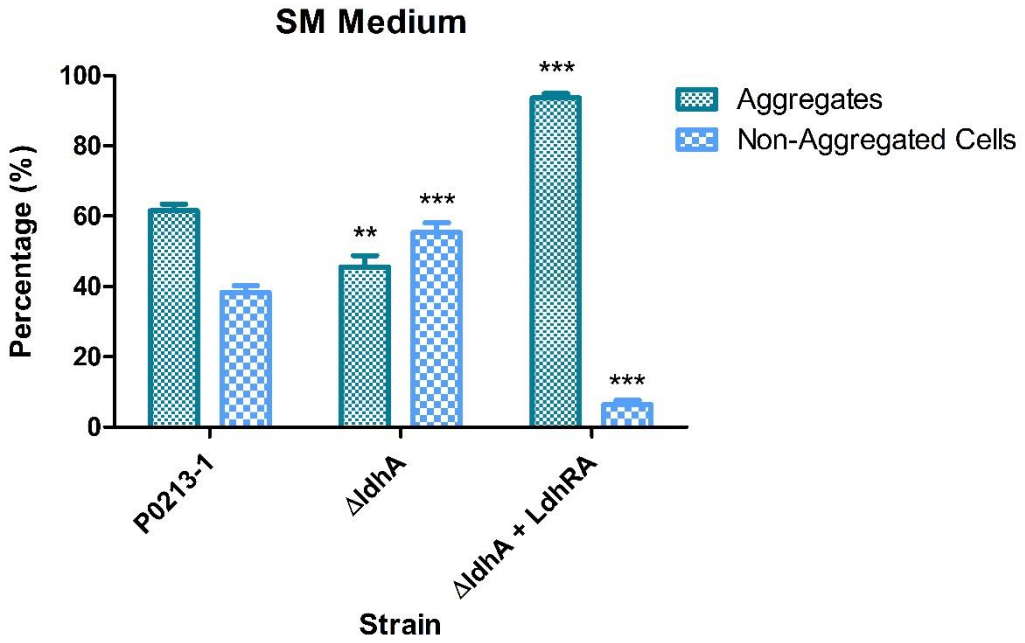

Figure 29 Dry weight results of P0213-1, *ΔldhA* and complemented mutant. Error bars represent the standard deviation of the means values of at least 3 replicates. Statistical significance of differences between P0213-1 and the remaining strains was determined by one-way ANOVA followed by Dunnett's multiple comparisons test. (**, *P*-value < 0.01; ***, *P*-value < 0.001).

4.4. Role of LdhA in biofilm formation

To evaluate whether the *ldhA* mutation also plays a role in surface attached biofilm formation, assays were conducted for the wild-type strain, Δ*ldhA* mutant and complemented mutant. Crystal violet staining of biofilms showed no differences between the wild-type and mutant, but the ability of the complemented mutant to produce biofilm was significantly higher (Figure 30). The phenotype of the mutant contrast with the one obtained by (Silva et al 2017) for *B. multivorans* ATCC 17616 which showed a reduction in the ability to form biofilms. Nevertheless, the fact that overexpression of *ldhA* gene increases the amount of biofilm is an indication that lactate dehydrogenase plays a role in biofilms.

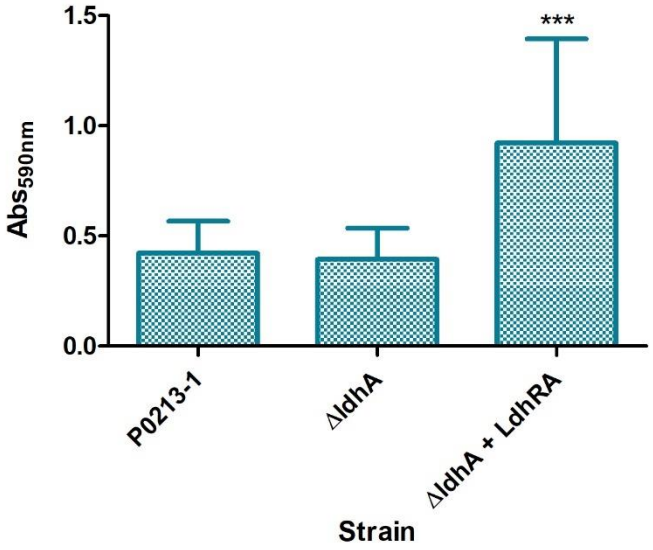

Figure 30 Biofilm formation of P0213-1 isolate, Δ*ldhA* mutant and complemented mutant, after 48h growth in polystyrene microplates at 37ºC. Error bars represent the standar deviation of the means values for at least 12 replicates. Statistical significance was determined by one-way ANOVA followed by Dunnett's multiple comparisons test. Differences were considered significant for P-values < 0.05. (***, *P*-value < 0.001).

4.5. Role of *ldhA* gene in exopolysaccharide production

Since mutation of *ldhR* and *ldhA* in *B. multivorans* ATCC 17616 had a positive effect in the production of exopolysaccharide, the same was evaluated for the strains under study. To do that, the wild-type, Δ*ldhA* mutant and complemented mutant were grown in SM medium for 48 hours. Then, the free cells supernatant was mixed with 3 volumes of ethanol to precipitate polysaccharides. Dry-weight determination confirmed the production of exopolysaccharide in the wild-type strain (Figure 31 A), but unexpectedly no polysaccharide was precipitated from the mutant and complemented mutant. Still, when both wild-type and mutant were grown in solid YEM, both displayed similar mucoid phenotype (Figure 31 B). At the moment we have no explanation for the differences between solid and liquid media regarding exopolysaccharide production.

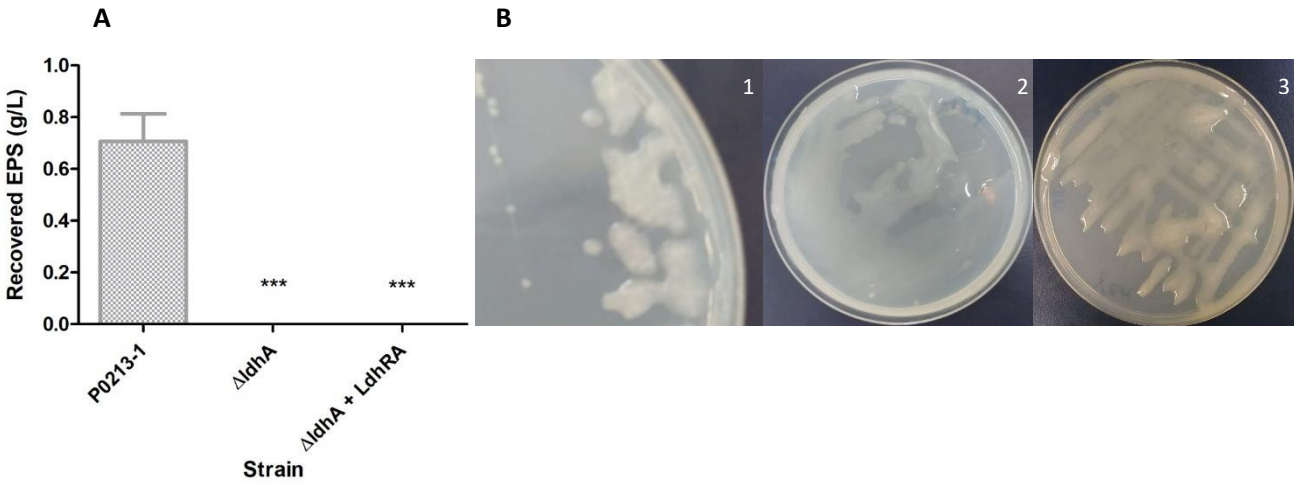

Figure 31 A- Exopolysaccharide production of wild-type P0213-1, Δ*ldhA* mutant and Δ*ldhA* complement, based on the dry weight of ethanol-precipitated EPS after 48h growth at 37ºC. Error bars correspond to the standard deviation of the mean values of three replicas. Statistical significance was determined by one-way ANOVA followed by Dunnett's multiple comparisons test. Differences were only considered significant for *P*-values<0.05. (***, *P*-value<0.001). **B** - Mucoid phenotype of P0213-1 (A), *ΔldhA* mutant (B) and complemented mutant (C) in yeast extract mannitol medium (YEM) after 48h incubation at 37ºC.

5. Evolution of the cellular aggregation trait under laboratory conditions

The aim of the following experiments was to observe if under laboratory settings free-living cells could evolve the cell aggregation phenotype, by growing them for many generations. The choice was isolate P0426-3, unable to form cell aggregates in SM medium. The experimental setting used was to grow this isolate in SM medium for 48 hours, 37ºC and 180 rpm and, then inoculate 1 ml culture into new medium for another 48 hours and so on up to 13 passages (30 days total). Before every passage, an aliquot was analysed under the microscope to search for the presence of cellular aggregates. Analysis of microscopy images showed cellular aggregation for the first time at day 7 (Figure 32). The size and shape of the aggregates remained more or less the same in the following days, but at the end of the experiment, aggregates were bigger and more compact. At the last time point, an aliquot was serially diluted and plated onto LB agar plates to obtain isolated colonies.

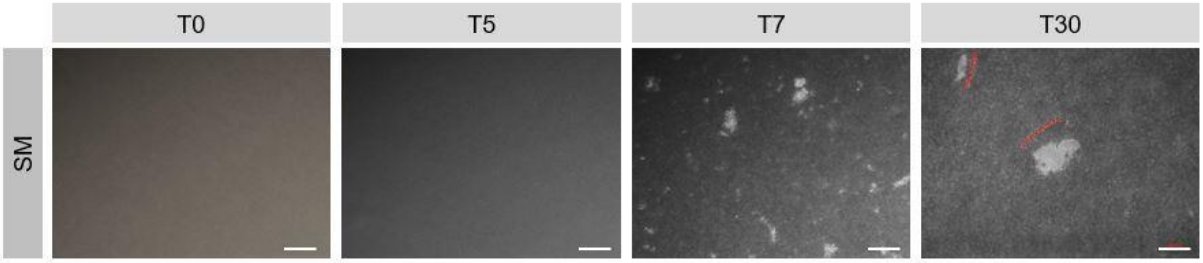

Figure 32 Microscopic images of non-aggregated cells and cellular aggregates of isolate P0426-3 during long-term evolution experiment. Images have a magnification of 100x and were obtained using ZEN software. White bars correspond to 100 µm (the used scale to measure the formed aggregates).

One colony showing distinct morphology, namely being very dry (Figure 33) was kept for confirmation of its ability to form aggregates. Figure 33 A confirms that strain named P0426-3T30 indeed produces aggregates of sizes that can go up to 40 µm.

Figure 33 Plate images of isolate P0426-3 before long-term evolution experiment (left) and after the 30 days long-term evolution experiment (right). It is possible to see that colonies from the evolved P0426-3 present a drier appearance. **A –** Microscopic images of P0426-3T30 strain. It has a magnification of 100x and was obtained using ZEN software. White bar corresponds to 100 µm scale.

To identify which mutations are present in this evolved mutant, we sequenced the whole genome by using Illumina technology. Since we already have the sequence of the ancestor P0426-3 (Pessoa

2017), here we performed a reference assembly by alignment of P0426-3T30 reads against P0426-3 genome, using aligner BWA-mem (Li et al. 2009). From this analysis we obtained several single nucleotide variants either in gene coding regions or intergenic regions as shown in Table 4. Three of the mutations mapped to Nodes (contigs) 4, 5 and 14 and, 8 mutations are in node 7. Two of the nonsynonymous mutations are found in a homologue of Bmul_5593, encoding a hypothetical protein and, in the *amiC* gene encoding N-acetylmuramyl-L-alanine amidase. The synonymous mutations are in gene *nlpD2* encoding a murein hydrolase activator and, the *flp* gene encoding a Tad-like Flp pilus-assembly family protein. Contrastingly to nonsynonymous mutations, synonymous (also called "silent mutations") mutations do not change the amino acid in the final protein. Nevertheless, they might influence the amount of protein being produced, either by modifying the stability of the transcript or by changing the codon usage, affecting the tRNA used during the translation process.

Table 4 Polymorphic genes identified among *B. multivorans* P0426-3 isolate recovered after the 30 days of long-term evolution experiment (Synonymous mutation – Syn; Non-synonymous – Nonsyn).

NODE	Position	Mutation	Gene Name	Annotation	Effect in protein	Effect of mutation
4	285529	G>C	*nlpD2*	Murein hydrolase Activatior	-	Syn
5	174949	G>C	*amiC*	*N*-acetylmuramyl-L-alanine amidase	L248R	Nonsyn
7	24021	T>C	*Flp*	Tad-like Flp pilus-assembly family protein	-	Syn
7	210873	C>A	Intergenic Region		-	-
7	210895	G>T				
7	210898	G>C				
7	210905	G>C				
7	210911	C>T				
7	210916	C>A				
7	210921	C>A				
7	210923	G>A				
14	10484	G>C	Bmul_5593	Hypothetical protein	G231R	Nonsyn

AmiC (*N*-acetylmuramyl-L-alanine amidase) is a peptidoglycan hydrolase responsible for the hydrolysation of the amide bond between Mur*N*Ac and L-alanine, separating by this the glycan strand from the peptide (Vollmer et al. 2008). These enzymes are also referred as peptidoglycan amidases or amidases. *N*-Acetylmuramyl-L-Alanine amidases (Mur*N*Ac-LAAs) are bacterial members of the autolytic system. These amidases carry a signal in their N-termini that enables their transport across the cytoplasmic membrane (Vollmer et al. 2008). Within bacterial proteome, many different Mur*N*Ac-LAAs are present. One of the identified Mur*N*Ac-LAAs is AmiC which has a periplasmic localization,

becoming soluble after the cleavage of the signal peptide (Vollmer et al. 2008). Like its homologues (AmiA and AmiB), AmiC plays an important role in cleaving the septum to release the new cells after cell division. The transport of AmiC to the septal ring is performed by the Twin-arginine transport (Tat) system. This system is responsible for the translocation of folded proteins containing cofactors across the bacterial cytoplasmatic membrane (Vollmer et al. 2008). Firstly, it was thought that AmiC did not contained a cofactor. However, after amino sequence comparisons of *Bacillus polymyxa* bacteriophage PSA it was suggested that AmiC and its homologous are Zn^{2+} containing metallo-enzymes (Korndörfer et al. 2006).

Because AmiC is involved in the process of septum cleavage which allows separation of daughter cells, so it is expected that differences in its expression and function would influence the capacity of cell division. Such facts were already observed by Vollmer *et al.* (Vollmer et al. 2008). In their study, it was observed that the *amiC* deletion mutant cells separate poorly during cell division. Due to this, between 20 and 30% of the cell population are in a chain form, composed by three up to six unseparated cells (Vollmer et al. 2008). It was also observed that other autolysins play an important role in the development of biofilms, being required for the formation of such structures (Heilmann et al. 1997).

However, to properly function, AmiC needs to be activated. Through direct protein-protein interactions with NlpD (a murein hydrolase activator), AmiC and other amidases activity, is controlled (Peters et al. 2013), enhancing it. NlpD is a member of the LytM family proteins which contains a LytM (peptidase M23) domain. NlpD is a lipoprotein with an *N*-terminal lipid moiety which serves as a membrane anchor (Yang et al. 2018). After its synthesis in the cytoplasm, the NlpD protein is transported to the periplasm where it anchors to the outer membrane with the *N*-terminus (Yang et al. 2018). This protein physically interacts with the peptidoglycan, being this interaction specific. Although being important for the separation of daughter cells, it was observed that in *E. coli* and in *Xanthomonas campestris* NlpD does not have by itself a peptidoglycan hydrolytic activity (Yang et al. 2018). NlpD influences cell division by modulating AmiC activity to hydrolase peptidoglycan, this is, activates AmiC activity (Yang et al. 2018), being its activity indispensable to a proper cell division.

Interestingly, in our evolved strain, P0426-3T30, both *nlpD* and *amiC* genes were mutated. Although, we cannot predict whether these mutations have positive or negative effects on enzyme activity, it is possible that they effect cell division, by preventing cells to separate. That way, they would stay together and form aggregates.

Beside the mutations in genes related to peptidoglycan degradation, namely in cell division, a gene related to the expression of the adhesive Flp (fimbrial low-molecular-weight protein) pili also suffered a mutation. This type of pili is synthesized by the products of *tad* genes (Tad from tight adherence). They encode a machinery known as the Tad macromolecular transport system, that is required for the assembly of the Flp pili (Tomich et al. 2007). The *tad* locus is composed of 14 different genes, being the first one (*flp-1* gene) the one which encodes the major structural component of Flp pili (Tomich et al. 2007). Between 12 to 13 of these genes are essential for Flp-pilus production, autoaggregation and biofilm formation (Kachlany et al. 2000; Kachlany et al. 2001). The expression of these genes,

depending on the species, varies with oxygen concentrations and quorum-sensing. *P. aeruginosa* Flp pili expression might be induced in the human host, especially when quorum-sensing pathways are activated (Tomich et al. 2007). Pili derived from the Tad macromolecular transport system can be composed of two possible types of prepilins (Type IVa and Type IVb). Type IVa prepilins have short *N*-terminal signal sequences (5-6 amino acids) and its mature proteins have 150 amino acids, whereas Type IVb prepilins have longer signal sequences (15-30 amino acids) and also larger mature forms (190 amino acids) (Tomich et al. 2007). All genes belonging to the *tad* locus are necessary to pili assembly. However, the most important one is *flp*-1. P0426-3T30 mutation that took place in this region did not changed the amino acid of the protein (synonymous). With this, it would be expected that no alterations in the protein function would happen. However, due to the stated above, the amount of protein being produced might be different. In this case, alterations in the production of pili and, as a consequence cell adhesion could be affected. Since we observed aggregates formation, it could be that these mutant cells display higher adhesion ability. Further studies need to be done to confirm or not this hypothesis.

Seven mutations were mapped into the same intergenic region (Figure 34). This region contains the promoter of a putative operonic structure with two genes encoding hypothetical proteins and a sodium proton antiporter. By affecting a promoter, these mutations might have strong impact on the expression of this operonic structure.

In *E. coli*, *nhaP* gene encodes a Na^+/H^+ antiporter (NhaP). Within bacterial cells this antiporter plays several important roles such as establishment of an electrochemical potential across membranes, extrusion of Na^+ which is toxic to cells when present in high concentrations, regulation of intracellular pH under alkaline conditions, and at last but not least, regulation of cell volume (Utsugi et al. 1998). Alteration in the expression of such protein might have strong effects on cell physiology. However, to understand if the observed mutations influence the expression of the downstream genes more tests and analysis should be performed.

Figure 34 Image of the intergenic region between *plcN2* and the hypothetical gene, where the mutations took place. The image was designed using SnapGene software (from GSL Biotech; available at snapgene.com).

At last, a hypothetical protein suffered a non-synonymous mutation, which means that the mutation changed the respective amino acid, and as a consequence the function of the protein can be compromised. Although the gene is not yet described, according to the String software (Szklarczyk et al. 2017) it is predicted to be an UBA/THIF-type NAD/FAD binding fold. This domain is a NAD/FAD-

binding fold that interferes in the activation of E1 enzyme (Ubiquitin-activating enzyme). The role of proteins with this motif in bacteria is unknown.

Together, we can conclude that our evolution experiment was successful, since by serial passages it was possible to evolve the cell aggregates phenotype. Mutations in a gene involved in the synthesis of pili and cell division might contribute to this phenotype.

6. Concluding remarks and future perspectives

The importance of cellular aggregation in CF pathogens is highlighted in studies showing that in the airways of CF patients these bacteria are often found in small clusters (Worlitzsch et al. 2002; Schwab et al. 2014). Also, Silva et al. (2017) has shown that environmental and clinical isolates of several Bcc species are able to form microscopic to macroscopic aggregates *in vitro.* Our hypothesis is that the establishment of a chronic infection requires adaptations, including cell aggregation, as a way to mitigate the stresses present in the CF lung.

This work started by analysing approximately 130 CF clinical isolates of *B. multivorans* for their ability to aggregate in SM medium. Data confirmed that the majority of the isolates do form aggregates and some who did not were late isolates within the longitudinal series. Then it was tested whether growth in a medium mimicking the nutrients found in the lungs would have an impact in cell aggregation. Interestingly, all tested isolates, even the ones unable to aggregate in SM medium, were able to form cellular aggregates. The search for environmental conditions triggering aggregates formation, revealed that sub-inhibitory concentrations of ciprofloxacin was the best trigger, increasing the biomass present as aggregates in most of the isolates. Other stresses such as hydrogen peroxide and osmotic stress had an effect, but it was isolate-specific. Together, our results confirmed an intrinsic ability of *B. multivorans* isolates to form cell aggregates and this can be enhanced by stress conditions similar to the ones found in the CF lung.

Previous studies have identified lactate dehydrogenase as important for aggregates formation both in *B. multivorans* (Silva et al 2017) and *Pseudomonas aeruginosa* (Petrova et al. 2012). Here, we want to evaluate whether this gene was also implicated in aggregates formation in *B. multivorans* P0213-1 clinical isolate. The *ldhA* mutant was successfully constructed, and its role in cellular aggregation confirmed. Interestingly, deletion of this gene decreased the biomass of aggregates, but its overexpression had stronger influence, with the amount of aggregates biomass increasing to more than 90%. We believed the importance of this protein might be with the fermentation of pyruvate into D-lactate within the hypoxic zones of the aggregate in order to obtain energy.

The last set of experiments performed aimed to evolve the aggregation phenotype under laboratory conditions and identify mutations that could be responsible for inducing that phenotype. By serial passages of isolate P0426-3 (which was growing as free cells) in SM medium we were able to trigger the aggregation phenotype at day 7 of the evolution experiment. Sequencing the genome of a colony obtained at day 30 allowed to identify several mutations when compared to the ancestor. These mutations mapped into genes affecting adhesion, cell division and hypothetical proteins. It is likely that some of them might be responsible for the observed phenotype.

This work gave some insights into the prevalence of the cellular aggregation trait in *B. multivorans* clinical isolates; identified some environmental triggers; confirmed the role of a metabolic enzyme in the formation of aggregates with increased size; and identified new putative genes with a role in the trait under study. Still, a lot of work has to be done, particularly by testing all *B. multivorans* clinical isolates in SCFM medium; confirming if the role of lactate dehydrogenase in cell aggregation is

through energy generation or if it is mediated by lactate signalling; repeat the evolution experiment with more replicates to identify other mutations; and analyse the role of Flp pilus in aggregates formation. Despite all we still have to discover, we believe that these multicellular structures might confer higher protection against the immune system and antimicrobial, thus enabling cells to persist.

7. References

Aaron, Shawn D, Wendy Ferris, Deborah A Henry, David P Speert, and Noni E M A C Donald. 2000. "Multiple combination bactericidal antibiotic testing for patients with cystic fibrosis infected with *Burkholderia cepacia*." *American Journal of Respiratory and Critical Care Medicine* 161 (16): 1206–12.

Allesen-Holm, Marie, Kim Bundvig Barken, Liang Yang, Mikkel Klausen, Jeremy S. Webb, Staffan Kjelleberg, Søren Molin, Michael Givskov, and Tim Tolker-Nielsen. 2006. "A characterization of DNA release in *Pseudomonas aeruginosa* cultures and biofilms." *Molecular Microbiology* 59 (4): 1114–28. doi:10.1111/j.1365-2958.2005.05008.x.

Anderson, Virginia E., Thomas D. Gootz, and Neil Osheroff. 1998. "Topoisomerase IV catalysis and the mechanism of quinolone action." *Journal of Biological Chemistry* 273 (28): 17879–85. doi:10.1074/jbc.273.28.17879.

Argenio, David a D, David a D Argenio, M Worth Calfee, M Worth Calfee, Paul B Rainey, Paul B Rainey, Everett C Pesci, and Everett C Pesci. 2002. "Autolysis and autoaggregation in *Pseudomonas aeruginosa* colony morphology mutants." *Microbiology* 184 (23): 6481–89. doi:10.1128/JB.184.23.6481.

Banin, Ehud, Michael L Vasil, and E Peter Greenberg. 2005. "Iron and *Pseudomonas aeruginosa* biofilm formation." *PNAS* 102 (31): 11076–81.

Bankevich, Anton, Sergey Nurk, Dmitry Antipov, Alexey A. Gurevich, Mikhail Dvorkin, Alexander S. Kulikov, Valery M. Lesin, et al. 2012. "SPAdes: A new genome assembly algorithm and its applications to single-cell sequencing." *Journal of Computational Biology* 19 (5): 455–77. doi:10.1089/cmb.2012.0021.

Behrends, V., J. G. Bundy, and H. D. Williams. 2011. "Differences in strategies to combat osmotic stress in *Burkholderia cenocepacia* elucidated by NMR-Based metabolic profiling." *Letters in Applied Microbiology* 52 (6): 619–25. doi:10.1111/j.1472-765X.2011.03050.x.

Bible, Amber N., Gurusahai K. Khalsa-Moyers, Tanmoy Mukherjee, Calvin S. Green, Priyanka Mishra, Alicia Purcell, Anastasia Aksenova, Gregory B. Hurst, and Gladys Alexandre. 2015. "Metabolic adaptations of *Azospirillum brasilense* to oxygen stress by cell-cell clumping and flocculation." *Applied and Environmental Microbiology* 81 (September): AEM.02782-15. doi:10.1128/AEM.02782-15.

Bible, Amber N., Bonnie B. Stephens, Davi R. Ortega, Zhihong Xie, and Gladys Alexandre. 2008. "Function of a chemotaxis-like signal transduction pathway in modulating motility, cell clumping, and cell length in the alphaproteobacterium *Azospirillum brasilense*." *Journal of Bacteriology* 190 (19): 6365–75. doi:10.1128/JB.00734-08.

Boes, Nelli, Kerstin Schreiber, Elisabeth Ha, Lothar Jaensch, and Max Schobert. 2006. "The *Pseudomonas aeruginosa* universal stress protein PA4352 is essential for surviving anaerobic

energy stress." *Journal of Bacteriology* 188 (18): 6529–38. doi:10.1128/JB.00308-06.

Borriello, Giorgia, Erin Werner, Frank Roe, Aana M Kim, Garth D Ehrlich, and Philip S Stewart. 2004. "Oxygen limitation contributes to antibiotic tolerance of *Pseudomonas aeruginosa* in biofilms" *Antimicrobial Agents and Chemotherapy* 48 (7): 2659–64. doi:10.1128/AAC.48.7.2659.

Brambilla, Cecilia, Marta Llorens-Fons, Esther Julián, Estela Noguera-Ortega, Cristina Tomàs-Martínez, Miriam Pérez-Trujillo, Thomas F. Byrd, Fernando Alcaide, and Marina Luquin. 2016. "Mycobacteria clumping increase their capacity to damage macrophages." *Frontiers in Microbiology* 7 (OCT): 1–12. doi:10.3389/fmicb.2016.01562.

Burdman, Saul, Edouard Jurkevitch, Boris Schwartsburd, Michal Hampel, and Yaacov Okon. 1998. "Aggregation in *Azospirillum brasilense*: effects of chemical and physical factors and involvement of extracellular components." *Microbiology* 144 (7): 1989–99. doi:10.1099/00221287-144-7-1989.

Cowan, J. 2002. "Structural and catalytic chemistry of magnesium dependent enzymes." *Biometals* 15: 225–235. doi:1016022730880.

Davies, D G, M R Parsek, J P Pearson, B H Iglewski, J W Costerton, E P Greenberg, J. R. Lawrence, et al. 1998. "The involvement of cell-to-cell signals in the development of a bacterial biofilm." *Science (New York, N.Y.)* 280 (5361): 295–98. doi:10.1126/science.280.5361.295.

Engman, Jakob, Olaspers Sara Eriksson, Sunil D Saroj, Leopold L Ilag, Ann-beth Jonsson, Nadezda Zguna, and Pilar Lloris-garcera. 2017. "Host cell-derived lactate functions as an effector Molecule in *Neisseria meningitidis* microcolony dispersal." *PLoS Pathogens* 13 (4): 1–27.

Ferreira, Ana S., Jorge H. Leitão, Sílvia A. Sousa, Ana M. Cosme, Isabel Sá-Correia, and Leonilde M. Moreira. 2007. "Functional analysis of *Burkholderia cepacia* Genes BceD and BceF, encoding a phospholyrosine phosphatase and a tyrosine autokinase, respectively: role in exopolysaccharide biosynthesis and biofilm formation." *Applied and Environmental Microbiology* 73 (2): 524–34. doi:10.1128/AEM.01450-06.

Ferreira, Ana S, Inês N Silva, Vítor H Oliveira, Raquel Cunha, and Leonilde M Moreira. 2011. "Insights into the role of extracellular polysaccharides in *Burkholderia* adaptation to different environments." *Frontiers in Cellular and Infection Microbiology* 1 (December): 1–9. doi:10.3389/fcimb.2011.00016.

Filkins, Laura M., and George A. O'Toole. 2015. "Cystic fibrosis lung infections: polymicrobial, complex, and hard to treat." *PLoS Pathogens* 11 (12): 1–8. doi:10.1371/journal.ppat.1005258.

Ghani, M, and J S Soothill. 1997. "Ceftazidime, gentamicin, and rifampicin, in combination, kill biofilms of mucoid *Pseudomonas aeruginosa.*" *Canadian Journal of Microbiology* 43 (11): 999–1004.

Goodman, Andrew L., Massimo Merighi, Mamoru Hyodo, Isabelle Ventre, Alain Filloux, and Stephen Lory. 2009. "Direct interaction between sensor kinase proteins mediates acute and chronic disease phenotypes in a bacterial pathogen." *Genes and Development* 23 (2): 249–59.

doi:10.1101/gad.1739009.

Haaber, Jakob, Marianne Thorup Cohn, Dorte Frees, Thorbjørn Joest Andersen, and Hanne Ingmer. 2012. “Planktonic aggregates of *Staphylococcus aureus* protect against common antibiotics.” *PLoS ONE* 7 (7): 1–12. doi:10.1371/journal.pone.0041075.

Hangas, Anu, Koit Aasumets, Nina J Kekäläinen, Mika Paloheinä, Jaakko L Pohjoismäki, Joachim M Gerhold, and Steffi Goffart. 2018. “Ciprofloxacin impairs mitochondrial DNA replication initiation through inhibition of Topoisomerase 2.” *Nucleic Acids Research* 46 (18): 9625–36. doi:10.1093/nar/gky793.

Hardalo, C, and S C Edberg. 1997. “*Pseudomonas aeruginosa*: assessment of risk from drinking water.” *Critical Reviews in Microbiology* 23 (1): 47–75. doi:10.3109/10408419709115130.

Harwood, Carolina Alvarez-Ortega and Caroline S. 2007. “Responses of *Pseudomonas aeruginosa* to low oxygen indicate that growth in the cystic fibrosis lung is by aerobic respiration.” *Mol Microbiol* 65 (1): 153–65. doi:10.1111/j.1365-2958.2007.05772.x.Responses.

Heilmann, Christine, Muzaffar Hussain, Georg Peters, and Friedrich Götz. 1997. “Evidence for autolysin-mediated primary attachment of *Staphylococcus epidermidis* to a polystyrene surface.” *Molecular Microbiology* 24 (5): 1013–24. doi:10.1046/j.1365-2958.1997.4101774.x.

Inês N. Silva,a Marcelo J. Ramires,a Lisa A. Azevedo,a Ana R. Guerreiro,a Andreia C. Tavares,a* Jörg D. Becker,b Leonilde M. Moreiraa, c. 2017. “Regulator LdhR and D-lactate dehydrogenase LdhA of *Burkholderia multivorans* play roles in carbon overflow and in planktonic cellular aggregate formation.” *Applied and Environmental Microbiology* 83 (19): 1–24.

Kachlany, S. C., P. J. Planet, M. K. Bhattacharjee, E. Kollia, R. DeSalle, D. H. Fine, and D. H. Figurski. 2000. “Nonspecific adherence by *Actinobacillus actinomycetemcomitans* requires genes widespread in bacteria and archaea.” *Journal of Bacteriology* 182 (21): 6169–76. doi:10.1128/JB.182.21.6169-6176.2000.

Kachlany, Scott C., Paul J. Planet, Rob DeSalle, Daniel H. Fine, David H. Figurski, and Jeffrey B. Kaplan. 2001. “Flp-1, the first representative of a new pilin gene subfamily, is required for non-specific adherence of *Actinobacillus actinomycetemcomitans*.” *Molecular Microbiology* 40 (3): 542–54. doi:10.1046/j.1365-2958.2001.02422.x.

Kearse, Matthew, Richard Moir, Amy Wilson, Steven Stones-Havas, Matthew Cheung, Shane Sturrock, Simon Buxton, et al. 2012. “Geneious basic: an integrated and extendable desktop software platform for the organization and analysis of sequence data.” *Bioinformatics* 28 (12): 1647–49. doi:10.1093/bioinformatics/bts199.

Korndörfer, Ingo P., Joseph Danzer, Mathias Schmelcher, Markus Zimmer, Arne Skerra, and Martin J. Loessner. 2006. “The crystal structure of the bacteriophage PSA endolysin reveals a unique fold responsible for specific recognition of *Listeria* cell walls.” *Journal of Molecular Biology* 364 (4): 678–89. doi:10.1016/j.jmb.2006.08.069.

Latifi, A, M.K. Winson, M. Foglino, B.W. Bycroft, G.S.A.B. Stewart, A. Lazdunski, and P. Williams. 1995. “Multiple homologs of Luxr and Luxl control expression of virulence determinants and secondary metabolites through quorum sensing in *Pseudomonas aeruginosa* Pao1.” *Molecular Microbiology* 17: 333–43. doi:10.1111/j.1365-2958.1995.mmi_17020333.x.

Li, Heng, Heng Li, Richard Durbin, and Richard Durbin. 2009. “Fast and accurate short read alignment with Burrows-Wheeler transform.” *Bioinformatics (Oxford, England)* 25 (14): 1754–60. doi:10.1101/gr.129684.111.

Medina, Gerardo, Katy Juárez, and Gloria Soberón-Chávez. 2003. “The *Pseudomonas aeruginosa* RhlAB operon is not expressed during the logarithmic phase of growth even in the presence of its activator RhlR and the autoinducer N-butyryl-homoserine lactone.” *Journal of Bacteriology* 185 (1): 377–80. doi:10.1128/JB.185.1.377-380.2003.

Mulcahy, Heidi, and Shawn Lewenza. 2011. “Magnesium limitation is an environmental trigger of the *Pseudomonas aeruginosa* biofilm lifestyle.” *PLoS ONE* 6 (8). doi:10.1371/journal.pone.0023307.

O’Sullivan, Brian P., and Steven D. Freedman. 2009. “Cystic Fibrosis.” *The Lancet* 373 (9678). *Elsevier* Ltd: 1891–1904. doi:10.1016/S0140-6736(09)60327-5.

Palmer, Kelli L., Lindsay M. Aye, and Marvin Whiteley. 2007. “Nutritional cues control *Pseudomonas aeruginosa* multicellular behavior in cystic fibrosis sputum.” *Journal of Bacteriology* 189 (22): 8079–87. doi:10.1128/JB.01138-07.

Paranjape, S.M., and P.J. Mogayzel Jr. 2014. “Cystic Fibrosis.” *Pediatrics in Review* 35 (5): 1992–2001. doi:10.1542/pir.35-5-194.

Passador, L, J M Cook, M J Gambello, L Rust, and B H Iglewski. 1993. “Expression of *Pseudomonas aeruginosa* virulence genes requires cell-to-cell communication.” *Science (New York, N.Y.)* 260: 1127–30. doi:10.1126/science.8493556.

Pesci, E. C., J. B. J. Milbank, J. P. Pearson, S. McKnight, A. S. Kende, E. P. Greenberg, and B. H. Iglewski. 1999. “Quinolone signaling in the cell-to-cell communication system of *Pseudomonas aeruginosa*.” *Proceedings of the National Academy of Sciences* 96 (20): 11229–34. doi:10.1073/pnas.96.20.11229.

Pessoa, Filipa Duarte. 2017. “Long-term evolution of *Burkholderia multivorans* bacteria during chronic respiratory infections of cystic fibrosis patients,” *Master Thesis, Instituto Superior Técnico*.

Peters, Nick T., Cécile Morlot, Desirée C. Yang, Tsuyoshi Uehara, Thierry Vernet, and Thomas G. Bernhardt. 2013. “Structure-function analysis of the LytM domain of EnvC, an activator of cell wall remodelling at the *Escherichia coli* division site.” *Molecular Microbiology* 89 (4): 690–701. doi:10.1111/mmi.12304.

Petrova, Olga E, Jill R Schurr, Michael J Schurr, and Karin Sauer. 2012. “Microcolony formation by the opportunistic pathogen *Pseudomonas aeruginosa* requires pyruvate and pyruvate fermentation.”

Molecular Microbiology 86 (4): 819–35. doi:10.1111/mmi.12018.

Sadasivan, L., and C. A. Neyra. 1985. “Flocculation in *Azospirillum brasilense* and *Azospirillum lipoferum*: exopolysaccharides and cyst formation.” *Journal of Bacteriology* 163 (2): 716–23.

Sagel, Scott D., Marci K. Sontag, Jeffrey S. Wagener, Robert K. Kapsner, Iris Osberg, and Frank J. Accurso. 2002. “Induced sputum inflammatory measures correlate with lung function in children with cystic fibrosis.” *The Journal of Pediatrics* 141 (6): 811–17. doi:10.1067/mpd.2002.129847.

Schreiber, Kerstin, Nelli Boes, Martin Eschbach, Lothar Jaensch, Juergen Wehland, Thomas Bjarnsholt, Michael Givskov, Morten Hentzer, and Max Schobert. 2006. “Anaerobic survival of *Pseudomonas aeruginosa* by pyruvate fermentation requires an Usp-Type stress protein.” *JOURNAL OF BACTERIOLOGY* 188 (2): 659–68. doi:10.1128/JB.188.2.659.

Schwab, Ute, Lubna H. Abdullah, Olivia S. Perlmutt, Daniel Albert, C. William Davis, Roland R. Arnold, James R. Yankaskas, et al. 2014. “Localization of *Burkholderia cepacia* complex bacteria in cystic fibrosis lungs and interactions with *Pseudomonas aeruginosa* in hypoxic mucus.” *Infection and Immunity* 82 (11): 4729–45. doi:10.1128/IAI.01876-14.

Seemann, Torsten. 2014. “Prokka: rapid prokaryotic genome annotation.” *Bioinformatics* 30 (14): 2068–69. doi:10.1093/bioinformatics/btu153.

Sriramulu, Dinesh D., Heinrich Lünsdorf, Joseph S. Lam, and Ute Römling. 2005. “Microcolony formation: A novel biofilm model of *Pseudomonas aeruginosa* for the cystic fibrosis Lung.” *Journal of Medical Microbiology* 54 (7): 667–76. doi:10.1099/jmm.0.45969-0.

Szklarczyk, Damian, John H. Morris, Helen Cook, Michael Kuhn, Stefan Wyder, Milan Simonovic, Alberto Santos, et al. 2017. “The STRING Database in 2017: quality-controlled protein-protein association networks, made broadly accessible.” *Nucleic Acids Research* 45 (D1): D362–68. doi:10.1093/nar/gkw937.

Tomich, Mladen, Paul J. Planet, and David H. Figurski. 2007. “The Tad Locus: postcards from the widespread colonization island.” *Nature Reviews Microbiology* 5 (5): 363–75. doi:10.1038/nrmicro1636.

Utsugi, Junko, Kei Inaba, Teruo Kuroda, Masaaki Tsuda, and Tomofusa Tsuchiya. 1998. “Cloning and sequencing of a novel Na+/H+ antiporter gene from *Pseudomonas aeruginosa*.” *Biochimica et Biophysica Acta - Gene Structure and Expression* 1398 (3): 330–34. doi:10.1016/S0167-4781(98)00058-X.

Vollmer, Waldemar, Bernard Joris, Paulette Charlier, and Simon Foster. 2008. “Bacterial peptidoglycan (murein) hydrolases.” *FEMS Microbiology Reviews* 32 (2): 259–86. doi:10.1111/j.1574-6976.2007.00099.x.

Whiteley, M, M G Bangera, R E Bumgarner, M R Parsek, G M Teitzel, S Lory, and E P Greenberg. 2001. “Gene expression in *Pseudomonas aeruginosa* biofilms.” *Nature* 413 (6858): 860–64.

doi:10.1038/35101627.

Workentine, Matthew L., Joe J. Harrison, Aalim M. Weljie, Vy A. Tran, Pernilla U. Stenroos, Valentina Tremaroli, Hans J. Vogel, Howard Ceri, and Raymond J. Turner. 2010. “Phenotypic and metabolic profiling of colony morphology variants evolved from *Pseudomonas fluorescens* biofilms.” *Environmental Microbiology* 12 (6): 1565–77. doi:10.1111/j.1462-2920.2010.02185.x.

Worlitzsch, Dieter, Robert Tarran, Martina Ulrich, Ute Schwab, Aynur Cekici, Keith C. Meyer, Peter Birrer, et al. 2002. “Effects of reduced mucus oxygen concentration in airway *Pseudomonas* infections of cystic fibrosis patients.” *Journal of Clinical Investigation* 109 (3): 317–25. doi:10.1172/JCI0213870.

Wyckoff, Timna J O, Brittany Thomas, Daniel J. Hassett, and Daniel J. Wozniak. 2002. “Static growth of mucoid *Pseudomonas aeruginosa* selects for non-mucoid variants that have acquired flagellum-dependent motility.” *Microbiology* 148 (11): 3423–30. doi:10.1099/00221287-148-11-3423.

Yang, Li Chao, Yong Liang Gan, Li Yan Yang, Bo Le Jiang, and Ji Liang Tang. 2018. “Peptidoglycan hydrolysis mediated by the amidase AmiC and its LytM activator NlpD is critical for cell separation and virulence in the phytopathogen *Xanthomonas campestris*.” *Molecular Plant Pathology* 19 (7): 1705–18. doi:10.1111/mpp.12653.

Yang, Liang, Kim B Barken, Mette E Skindersoe, Allan B Christensen, Michael Givskov, Tim Tolker-nielsen, and Tim Tolker-nielsen. 2017. “Effects of iron on DNA release and biofilm development by *Pseudomonas aeruginosa*.” *Microbiology*, no. 2007: 1318–28. doi:10.1099/mic.0.2006/004911-0.

Yoon, Sang Sun, Robert F Hennigan, George M Hilliard, Urs A Ochsner, Kislay Parvatiyar, Moneesha C Kamani, Holly L Allen, et al. 2002. “P*seudomonas aeruginosa* anaerobic respiration in biofilms : relationships to cystic fibrosis pathogenesis” *Developmental Cell* 3: 593–603.

Zhang, Qiucen, Guillaume Lambert, David Liao, Hyunsung Kim, Kristelle Robin, Chih Kuan Tung, Nader Pourmand, and Robert H. Austin. 2011. “Acceleration of emergence of bacterial antibiotic resistance in connected microenvironments.” *Science* 333 (6050): 1764–67. doi:10.1126/science.1208747.

Zlosnik, James E A, Trevor J. Hird, Monica C. Fraenkel, Leonilde M. Moreira, Deborah A. Henry, and David P. Speert. 2008. “Differential mucoid exopolysaccharide production by members of the *Burkholderia cepacia* complex.” *Journal of Clinical Microbiology* 46 (4): 1470–73. doi:10.1128/JCM.02273-07.